# On electromagnetic instabilities at ultra-relativistic shock waves

Martin Lemoine, Guy Pelletier

Monthly Notices
of the
ROYAL ASTRONOMICAL SOCIETY

Mon. Not. R. Astron. Soc. **402,** 321–334 (2010) doi:10.1111/j.1365-2966.2009.15869.x

# On electromagnetic instabilities at ultra-relativistic shock waves

Martin Lemoine[1⋆] and Guy Pelletier[2⋆]

[1]*Institut d'Astrophysique de Paris, CNRS, UPMC, 98 bis boulevard Arago, F-75014 Paris, France*
[2]*Laboratoire d'Astrophysique de Grenoble, CNRS, Université Joseph Fourier II, BP 53, F-38041 Grenoble, France*

Accepted 2009 October 14. Received 2009 September 2; in original form 2009 April 22

**ABSTRACT**

Recent work on Fermi acceleration at ultra-relativistic shock waves has demonstrated the need for strong amplification of the background magnetic field on very short scales. Amplification of the magnetic field by several orders of magnitude has also been suggested by observations of gamma-ray bursts afterglows, both in downstream and upstream plasmas. This paper addresses this issue of magnetic field generation in a relativistic shock precursor through micro-instabilities. In a generic superluminal configuration, the level of magnetization of the upstream plasma turns out to be a crucial parameter, notably because the length scale of the shock precursor is limited by the Larmor rotation of the accelerated particles in the background magnetic field and by the speed of the shock wave. We discuss in detail and calculate the growth rates of the following beam plasma instabilities seeded by the accelerated and reflected particle populations: for an unmagnetized shock, the Weibel and filamentation instabilities, as well as the Čerenkov resonant instabilities with electrostatic modes; for a magnetized shock, the Weibel instability and the resonant Čerenkov instabilities with the longitudinal electrostatic modes, as well as the Alfvén, Whisler and extraordinary modes. All these instabilities are generated upstream, then they are transmitted downstream. The modes excited by Čerenkov resonant instabilities take on particular importance with respect to the magnetization of the downstream medium since, being plasma eigenmodes, they have a longer lifetime than the Weibel modes. We discuss the main limitation of the wave growth associated with the length of precursor and the magnetization of the upstream medium for both oblique and parallel relativistic shock waves. We also characterize the proper conditions to obtain Fermi acceleration at ultra-relativistic shock waves: for superluminal shock waves, the Fermi process works for values of the magnetization parameter below some critical value, and there is an intrinsic limitation of the achievable cosmic ray energy depending on the ratio of the magnetization to its critical value. We recover results of most recent particle-in-cell simulations and conclude with some applications to astrophysical cases of interest. In particular, Fermi acceleration in pulsar winds is found to be unlikely whereas its development appears to hinge on the level of upstream magnetization in the case of ultra-relativistic gamma-ray burst external shock waves.

**Key words:** acceleration of particles – shock waves – cosmic rays.



## 1 INTRODUCTION

Substantial progress has been accomplished in this last decade on our theoretical understanding of the acceleration of particles at relativistic shocks, revealing in more than one place crucial differences with Fermi acceleration at non-relativistic shock waves. For instance, Gallant & Achterberg (1999) and Achterberg et al. (2001) have emphasized the strong anisotropy of the cosmic ray population propagating upstream, which is directly related to the fact that the relativistic shock wave is always trailing right behind the accelerated particles. These particles are confined into a beam of opening angle $\theta \lesssim 1/\Gamma_{\rm sh}$ (with $\Gamma_{\rm sh}$ the Lorentz factor of the shock wave in the upstream frame) and are overtaken by the shock wave on a time-scale $r_{\rm L}/\Gamma_{\rm sh}$, with $r_{\rm L}$ the typical Larmor radius of these particles in the background magnetic field. One consequence of the above is to restrict the energy gain per up → down → up cycle, $\Delta E/E$, to a factor of order unity. Early Monte Carlo numerical experiments, none the less, observed efficient Fermi acceleration, with a generic spectral index $s = 2.2$–$2.3$ in the ultra-relativistic limit (Bednarz & Ostrowski 1998; Achterberg et al. 2001; Lemoine & Pelletier 2003; Ellison & Double 2004), in agreement with

⋆E-mail: lemoine@iap.fr (ML); guy.pelletier@obs.ujf-grenoble.fr (GP)

semi-analytical studies (Kirk et al. 2000) and analytical calculations (Keshet & Waxman 2005). This value of the spectral index is, however, restricted to the assumption of isotropic turbulence both upstream and downstream of the shock (Niemiec & Ostrowski 2004; Lemoine & Revenu 2006), whereas the shock crossing conditions imply a mostly perpendicular magnetic field downstream, which severely limits the possibility of downstream scattering. Furthermore, it was later stressed by Niemiec & Ostrowski (2006) and Lemoine, Pelletier & Revenu (2006) that these early studies implicitly ignored the correlation between the upstream and downstream particle trajectories during a cycle. In particular, the former numerical study demonstrated that Fermi acceleration became inefficient if the proper shock crossing conditions were applied to the background magnetic field. This result was demonstrated analytically in the latter study, concluding that Fermi acceleration could only proceed if strong turbulence ($\delta B \gg B$) existed on a scale much smaller than the typical larmor radius. The addition of turbulence on large scales $\gg r_{\rm L}$ does not help in this respect, as the particle then experiences a roughly coherent field on the short length scales that it probes during its cycle. Further studies by Niemiec, Ostrowski & Pohl (2006) have confirmed that Fermi acceleration proceeds if short-scale turbulence is excited to high levels, either downstream or upstream. The detailed conditions under which Fermi acceleration can proceed have been discussed analytically in Pelletier, Lemoine & Marcowith (2009); they are found to agree with the numerical results of Niemiec et al. (2006).

Amplification of magnetic fields on short spatial scales thus appears to be an essential ingredient in Fermi processes at ultra-relativistic shock waves. Quite interestingly, strong amplification has been inferred from the synchrotron interpretation of gamma-ray burst afterglows, downstream at the level of $\delta B/B \gtrsim 10^4$–$10^5$ (Waxman 1997; see Piran 2005 for a review), and upstream with $\delta B/B \gtrsim 10^2$–$10^3$ (Li & Waxman 2006), assuming an upstream magnetic field typical of the interstellar medium. Understanding the mechanism by which the magnetic field gets amplified is crucial to our understanding to relativistic Fermi acceleration, since the nature of this short-scale turbulence will eventually determine the nature of scattering, hence the spectral index and the acceleration time-scale.

Concerning the amplification of the downstream magnetic field, the Weibel two stream instability operating in the shock transition layer has been considered as a prime suspect (Gruzinov & Waxman 1999; Medvedev & Loeb 1999; Wiersma & Achterberg 2004; Lyubarsky & Eichler 2006; Achterberg & Wiersma 2007; Achterberg, Wiersma & Norman 2007). Several questions nevertheless remain open. For instance, Hededal & Nishikawa (2005) and Spitkovsky (2005) have observed, by the means of numerical simulations that this instability gets quenched when the magnetization of the upstream field becomes sufficiently large. On analytical grounds, Wiersma & Achterberg (2004), Achterberg & Wiersma (2007) and Lyubarsky & Eichler (2006) have argued that it saturates at a level too low to explain the gamma-ray burst afterglow. The long-term evolution of the generated turbulence also remains an open question, although Medvedev et al. (2005) claim to see the merging of current filaments into larger filaments through dedicated numerical experiments.

Regarding upstream instabilities, the relativistic generalization of the non-resonant Bell instability has been investigated by Milosavljević & Nakar (2006) and Reville, Kirk & Duffy (2006) in the case of parallel shock waves. However, ultra-relativistic shock waves are generically superluminal, with an essentially transverse magnetic field in the shock front. For this latter case, Pelletier et al. (2009) have shown that the equivalent of the Bell non-resonant instability excites magnetosonic compressive modes and saturates at a moderate level $\delta B/B \sim 1$ in the frame of the linear theory.

In recent years, particle-in-cell (PIC) simulations have become a key tool in the investigation of these various issues. Such simulations go (by construction) beyond the test particle approximation and may therefore probe the wave – particle relationship, which is central to all of the above issues. Of course, such benefice comes at the price of numerical limitations of the simulations, both in terms of dimensionality and of dynamic range, which in turns impact on the mass ratios accessible to the computation. None the less, early PIC simulations have been able to simulate the interpenetration of relativistic flows and to study the development of two stream instabilities at early times, see e.g. Silva et al. (2003), Frederiksen et al. (2004), Hededal et al. (2004), Dieckmann (2005), Dieckmann, Drury & Shukla (2006a), Dieckmann, Shukla & Drury (2006b), Nishikawa et al. (2006, 2007) and Frederiksen & Dieckmann (2008) for unmagnetized colliding plasma shells, and Nishikawa et al. (2003), Dieckmann, Eliasson & Shukla (2004a,b), Nishikawa et al. (2005) and Hededal & Nishikawa (2005) for studies of the magnetized case. The formation of the shock itself has been observed for both electron–positron and electron–proton plasmas thanks to recent simulations that were able to carry the integration on to longer time-scales, see e.g. Spitkovsky (2005), Kato (2007), Chang, Spitkovsky & Arons (2008), Dieckmann, Shukla & Drury (2008), Spitkovsky (2008a,b) and Keshet et al. (2009). All of the above studies use different techniques for the numerical integration, and varying parameters (dimensions, composition, mass ratios, density ratios of the colliding plasmas and relative Lorentz factors) in order to examine different aspects of the instabilities to various degrees of accuracy and over different time-scales.

Several of these studies have reported hints for particle acceleration through non-Fermi processes (Dieckmann et al. 2004b; Frederiksen et al. 2004; Hededal et al. 2004; Hededal & Nishikawa 2005; Nishikawa et al. 2005; Dieckmann et al. 2006b, 2008). Concrete evidence for Fermi acceleration, i.e. particles bouncing back and forth across the shock wave has come with the recent simulations of Spitkovsky (2008b), and was studied in more details for both magnetized and unmagnetized shock waves in Sironi & Spitkovsky (2009). In particular, this latter study has demonstrated the inefficiency of Fermi acceleration at high upstream magnetization in the superluminal case, along with the absence of amplification of the magnetic field (thus in full agreement with the calculations of Lemoine et al. 2006). This result is particularly interesting because it suggests that the magnetization of the upstream plasma, in limiting the length of the precursor, may hamper the growth of small-scale magnetic fields, and therefore inhibit Fermi cycles. Finally, the long-term simulations of Keshet et al. (2009) have also observed a steady development of turbulence upstream of the shock wave, suggesting that as time proceeds, particles are accelerated to higher and higher energies and may thus stream further ahead of the shock wave. We will discuss this issue as well at the end of the present work.

The main objective of this paper is to undertake a systematic study of micro-instabilities in the upstream medium of a relativistic shock wave. We should emphasize that we assume the shock structure to exist and we concentrate our study on the shock transition region where the incoming upstream plasma collides with the shock reflected and shock accelerated ions that are moving towards upstream infinity. Therefore, care should be taken when confronting the present results to the above numerical simulations which reproduce the collision of two neutral plasma flows in order to study the

development of instabilities that eventually lead to the formation of the shock (through the thermalization of the electron and ion populations). The physical set-up that we have in mind matches best that obtained in the simulations of shock formation and particle acceleration described in Spitkovsky (2008b), Keshet et al. (2009) and Sironi & Spitkovsky (2009), or that simulated in Dieckmann et al. (2004a,b) and Frederiksen & Dieckmann (2008), or that studied in Medvedev & Zakutnyaya (2009). Our approach also rests on the following observation, namely that in the ultra-relativistic limit, the accelerated (or the reflected) particle population essentially behaves as an unmagnetized cold beam of Lorentz factor $\sim \Gamma_{\rm sh}^2$.

In the present paper, we assume the beam to be carrying a weak current and in so doing, we neglect electromagnetic current instabilities. We will nevertheless include in our summary of instabilities the relativistic generalization of the Bell current instability (Bell 2004), since it has been studied in detail in several recent studies (Milosavljević & Nakar 2006; Reville et al. 2006). The instability triggered by the cosmic ray current in the case of oblique shock waves has also been discussed in the relativistic regime in Pelletier et al. (2009). Note also that in the case of pair plasmas, electromagnetic current instabilities do not take place as the beam remains neutral.

The layout of the present paper is as follows. We examine the instabilities triggered by this beam, considering in turn the cases of an unmagnetized upstream plasma (Section 3) and that of a magnetized plasma (Section 4). In Section 5, we discuss the intermediate limit and construct a phase diagram indicating which instability prevails as a function of shock Lorentz factor and magnetization level. We then discuss the possibility of Fermi acceleration in the generated turbulence and apply these results to the case of gamma-ray bursts shock waves and pulsar winds. We will recover the trend announced above, namely that a magnetized upstream medium inhibits the growth of the magnetic field hence particle acceleration. In Section 2, we first discuss the general structure of a collisionless shock, in the case of an electron–proton plasma with a quasi-perpendicular mean field, borrowing from analyses in the non-relativistic limit.

## 2 GENERAL CONSIDERATIONS

### 2.1 On the configuration of a relativistic collisionless shock wave

A collisionless shock is built with the reflection of a fraction of incoming particles at some barrier, generally of electrostatic or magnetic nature. Let us sketch the general picture, borrowing from model of non-relativistic collisionless electro-ion shocks (see e.g. Treumann & Jaroschek 2008a,b for recent reviews). In an electron–proton plasma carrying an oblique magnetic field, one expects a barrier of both electrostatic and magnetic nature to rise. Because the magnetic field is frozen in most part of the plasma, its transverse component is amplified by the velocity decrease. This in itself forms a magnetic barrier which can reflect back a fraction of the incoming protons. Similarly, the increase of electron density together with the approach of the electron population towards statistical equilibrium is concomitant with the rise of an electrostatic potential such that $e\Phi \simeq T_{\rm e}\log(n/n_{\rm u|sh})$($n$ is the local density in the front frame, and $n_{\rm u|sh}$ the upstream incoming density viewed in the front frame). The electron temperature is expected to grow to a value comparable to, but likely different from that of protons, which reaches $T_{\rm p} \sim (\Gamma_{\rm sh}-1)m_{\rm p}\,c^2$. The electrostatic barrier thus allows the reflection of a significant part of the incoming protons since $e\Phi \sim (\Gamma_{\rm sh}-1)m_{\rm p}c^2$. Although it reflects a fraction of protons, it favours the transmission of electrons that would otherwise be reflected by the magnetic barrier. The reflection of a fraction of the protons ensures the matter flux preservation against the mass density increase downstream. However because the magnetic field is almost transverse, an intense electric field $E = \beta_{\rm sh}B$ energizes these reflected protons such that they eventually cross the barrier. Interactions between the different streams of protons are then expected to generate a turbulent heating of the proton population, which takes place mostly in the so-called 'foot' region. This foot region extends from the barrier upstream over a length scale (in the shock front frame, as indicated by the $_{|\rm sh}$ subscript) $\ell_{\rm F|sh} = r_{\rm L|sh}$, where $r_{\rm L|sh}$ denotes the Larmor radius of the reflected protons.

Entropy production in the shock transition region comes from two independent anomalous (caused by collisionless effects) heating processes for electrons and ions. The three ion beams in the foot (incoming, reflected in the foot and accelerated) interact through the 'modified two stream instability', which seemingly constitutes the main thermalization process of the ion population. A careful description of these anomalous heating processes certainly requires an appropriate kinetic description. For the time being, we note that the growth of the ion temperature develops on a length scale $\ell_{\rm F}$. The temperature of the electrons rather grows on a very short scale $\ell_{\rm R} \ll \ell_{\rm F}$ which defines the 'ramp' of the shock. In non-relativistic shocks, electrons reach a temperature larger than ions; however, we do not know yet whether this is the case in relativistic shocks. These electrons also experience heating in the convection electric field. Moreover, due to the strong gradient of magnetic field, an intense transverse electric current is concentrated, inducing anomalous heat transfer through the ramp. Probably an anomalous diffusion of electron temperature occurs that smoothes out the temperature profile; however, it has not been identified in relativistic shocks. Electron heating is described by the Ohm's law in the direction of the convection electric field (in the $\boldsymbol{x}\times\boldsymbol{B}$ direction, taken to be $z$),

$$\beta_x B + E = \frac{\eta c}{4\pi}\frac{{\rm d}B}{{\rm d}x}, \tag{1}$$

with $\beta_x < 0$ in the shock front frame, $E = \beta_{\rm sh}B_{\rm u}$, $B_{\rm u}$ denoting the background magnetic field at infinity. The magnetic field profile can be obtained by prescribing a velocity profile going from $-\beta_{\rm sh}c \sim -c$ to $\simeq -c/3$ over a distance much larger than $\ell_{\rm R}$. The profile displays a ramp at scale $\ell_{\rm R}$ followed by an overshoot before reaching the asymptotic value $3B_{\rm u}$. The above result indicates that the relevant scale for $\ell_{\rm R}$ is the relativistic resistive length,

$$\ell_{\rm R} \sim \frac{\eta c}{4\pi} = \delta_{\rm e}\frac{\nu_{\rm eff}}{\omega_{\rm pe}}. \tag{2}$$

This is a very short scale not larger than the electron inertial length $\delta_{\rm e} \equiv c/\omega_{\rm pe}$ even when the anomalous resistivity is so strong that the effective collision frequency $\nu_{\rm eff}$ is of order $\omega_{\rm pe}$. This scale thus represents the growth scale of three major quantities, namely, the potential, the magnetic field and the electron temperature. It is of interest to point out that this scale always remains much smaller than the foot scale. Indeed, even if $\delta_{\rm e}$ is estimated with ultra-relativistic electrons of relativistic mass $\Gamma_{\rm sh}m_{\rm p}$, i.e. $\delta_{\rm e} = [\Gamma_{\rm sh}m_{\rm p}c^2/(4\pi n_{e|\rm u}e^2)]^{1/2}$, it remains smaller than the foot length, since

$$\frac{\delta_{\rm e}}{\ell_{\rm F|sh}} = \left(\frac{B_{|\rm sh}^2}{4\pi n_{e|\rm u}\Gamma_{\rm sh}^2 m_{\rm p}c^2}\right)^{1/2} \ll 1, \tag{3}$$

using the value of $\ell_{\rm F|sh}$ for particles with typical energy $\Gamma_{\rm sh}m_{\rm p}c^2$ in the shock front. The last inequality in the above equation is a natural requirement for a strong shock. The downstream flow results from the mixing of the flow of first crossing ions (adiabatically slowed

down) with the flow of transmitted ions after reflection. All the ingredients of a shock are then realized.

In the case of an electron–positron plasma, when a magnetic field is considered, no electrostatic barrier rises, only the magnetic barrier appears. However, if the mean magnetic field is negligible, a barrier can rise only through the excitation of waves, as demonstrated by the PIC simulations discussed above.

The structure is thus described by two scales $\ell_{\rm R}$ and $\ell_{\rm F}$ and three small parameters: $\xi_{\rm cr}$, the fraction of thermal energy density behind the shock converted into cosmic ray energy, $\sigma_B$ the ratio of magnetic energy density over the incoming energy density and $1/\Gamma_{\rm sh}$.

### 2.2 Particle motion

As mentioned above, there are three particle populations in the foot: the cold incoming particles, the reflected protons and the accelerated particle population which has undergone at least one up , $\rightarrow$ down $\rightarrow$ up cycle. This latter population arrives upstream with a typical Lorentz factor of $\Gamma_{\rm b} \sim \Gamma_{\rm sh}^2$, with a typical relative spread of order unity. The second population of reflected protons also carries an energy $\simeq\Gamma_{\rm sh}^2 m_{\rm p}c^2$, since these particles have performed a Fermi-like cycle, albeit in the front rather than downstream. Therefore, one can treat these two populations as a single beam. From the point of view of the instabilities, one can approximate this beam as cold, with momentum distribution $\propto \delta(p_x - \Gamma_{\rm sh}^2 m_{\rm p}c)\delta(p_\perp)$. Indeed, the instabilities are governed by the beam velocity, the dispersion of which remains very small, being of order $\Delta\beta_{\rm b} \sim -(2/\Gamma_{\rm b}^2)\Delta\Gamma_{\rm b}/\Gamma_{\rm b}$. In order to verify this, one writes the susceptibility of the beam, assuming as above that it is unmagnetized on the scale of the instabilities (Melrose 1986),

$$\chi_{ij}^{\rm b} = -\frac{4\pi e^2}{m_{\rm p}\omega^2}\int \frac{{\rm d}^3 p}{\gamma}\, f_{\rm b}(\boldsymbol{p}) \times \left[\delta_{ij} + \frac{k_i c\beta_j + k_j c\beta_i}{\omega - \boldsymbol{k}\cdot\boldsymbol{\beta}c} + \frac{(k^2c^2-\omega^2)\beta_i\beta_j}{(\omega-\boldsymbol{k}\cdot\boldsymbol{\beta}c)^2}\right], \quad (4)$$

with $p = \beta\gamma m_{\rm p}c$ and $f_{\rm b}(\boldsymbol{p})$ the distribution function of the beam. Since the velocity distribution of the beam is essentially delta like, one may then indeed approximate the above beam susceptibility with that of a cold beam; the difference amounts to a redefinition of the beam plasma frequency by a factor of order unity.

Another crucial length scale in our study is the length scale of the precursor. As discussed above, this length scale $\ell_{\rm F|sh} = r_{\rm L|sh}$ in the front shock in the case of a magnetized shock wave. In the upstream frame, this can be rewritten as

$$\ell_{\rm F|u} \simeq \frac{r_{\rm L|u}}{\Gamma_{\rm sh}^3} = \frac{c}{\omega_{\rm ci}\Gamma_{\rm sh}\sin\theta_B} \quad (B_{\rm u} \neq 0). \quad (5)$$

We assume that the field is almost perpendicular in the front frame, but in the upstream comoving frame we consider its obliquity (angle $\theta_B$ with respect to the shock normal), assuming that $\sin\theta_B > 1/\Gamma_{\rm sh}$. The particular case of a parallel shock wave for which $\Gamma_{\rm sh}\sin\theta_B < 1$ is discussed in Section 5.2; there it will be shown that a fraction $(1-\Gamma_{\rm sh}\,\theta_B)^2$ of the particles that return upstream may actually propagate to upstream infinity in the limit of a fully coherent upstream magnetic field, while equation (5) remains correct for the rest of the accelerated particle population. The size of the precursor for the particles that escape away is eventually given by the level of turbulence ahead of the shock wave.

In the case of an unmagnetized shock wave, the size of the precursor is determined by the length travelled by the reflected protons in the self-generated short-scale turbulence. Neglecting for simplicity the influence of the short-scale upstream electric fields (we will see in Section 6 that this does not affect the following result), this length scale can be written (Milosavljević & Nakar 2006; Pelletier et al. 2009):

$$\ell_{\rm F|u} \simeq \frac{r_{\rm L|u}^2}{\Gamma_{\rm sh}^4\ell_{\rm c}} \simeq \frac{c^2}{\omega_{\rm ci}^2\ell_{\rm c}}, \quad (6)$$

where $\ell_{\rm c}$ represents the typical scale of short-scale magnetic fluctuations. Whether one or the other formula applies depends on several possible situations and outcomes: if the shock is magnetized and one considers the first generation of cosmic rays, one should use equation (5); if the shock is magnetized and one assumes that a stationary state has developed with strong self-generated turbulence, one should use equation (6); obviously, if the development of the turbulence cannot take place, one should rather use equation (5); finally, for an unmagnetized shock, equation (6) applies. In the following, we discuss the turbulence growth rate for these different cases.

There seems to be a consensus according to which magnetic fluctuations have to be tremendously amplified through the generation of cosmic rays upstream in order for Fermi acceleration to proceed. A fraction $\xi_{\rm cr}$ of the incoming energy is converted into cosmic rays and a fraction of this cosmic rays energy is converted into electromagnetic fluctuations, which add up to a fraction $\xi_{\rm em}$ of the incoming energy. This process is expected to develop such that the generation of cosmic rays allows the generation of electromagnetic waves that in turn, through more intense scattering, allows further cosmic ray acceleration and so on until some saturation occurs. We write the quantities $\xi_{\rm cr}$ and $\xi_{\rm em}$ as

$$\xi_{\rm cr} \equiv \frac{P_{\rm cr}}{\Gamma_{\rm sh}^2 n_{\rm u} m_{\rm p}c^2}, \quad \xi_{\rm em} \equiv \frac{U_{\rm em}}{\Gamma_{\rm sh}^2 n_{\rm u} m_{\rm p}c^2}, \quad (7)$$

with $\xi_{\rm em} < \xi_{\rm cr}$. We approximate the beam pressure with that of the cosmic rays, i.e. $P_{\rm cr} \approx \Gamma_{\rm sh} n_{\rm b|sh} m_{\rm p}c^2$ for the first generation of accelerated particles, as expressed in the shock front frame. The electromagnetic energy density is written $U_{\rm em}$ in the same frame, as usual.

Unless otherwise noted, our discussion takes place in the upstream rest frame in what follows.

## 3 UPSTREAM INSTABILITIES IN THE ABSENCE OF A MEAN MAGNETIC FIELD

When the ambient magnetic field can be neglected or is absent, the reflected particles and the fraction of particles that participate to the first Fermi cycle constitute a relativistic cold beam that pervades the ambient plasma and trigger three major micro-instabilities. One is the two stream electrostatic instability, which amplifies the electrostatic Langmuir field through a Čerenkov resonant interaction $\omega - \boldsymbol{k}\cdot\boldsymbol{v}_{\rm b} = 0$, with $\boldsymbol{k} \parallel \boldsymbol{E} \parallel \boldsymbol{v}_{\rm b}$. Another is the Weibel instability, with $\boldsymbol{k} \parallel \boldsymbol{v}_{\rm b} \perp \boldsymbol{E}$ and its analogue filamentation instability, with $\boldsymbol{k} \perp \boldsymbol{v}_{\rm b} \parallel \boldsymbol{E}$ (Bret, Firpo & Deutsch 2004, 2005a,b; see also Bret 2009 for a recent compilation). These two instabilities are non-resonant and mostly electromagnetic with a low phase velocity so that the magnetic component of the wave is dominant. It is thus particularly relevant for developing particle scattering. Finally, these authors have also discovered an oblique resonance which grows faster than the above two. It is mostly longitudinal (see further below) but $\boldsymbol{k}$ is neither perpendicular nor parallel to the beam. These growth rates are easily recovered as follows.

For a cold beam, equation (4) gives the following susceptibility:

$$\chi^{\rm b}_{ij} = -\frac{\omega^2_{\rm pb}}{\omega^2}\left[\delta_{ij} + \frac{k_i c\beta_{{\rm b}j} + k_j c\beta_{{\rm b}i}}{\omega - \boldsymbol{k}\cdot\boldsymbol{\beta}_{\rm b}c} + \frac{(k^2c^2-\omega^2)\beta_{{\rm b}i}\beta_{{\rm b}j}}{\left(\omega - \boldsymbol{k}\cdot\boldsymbol{\beta}_{\rm b}c\right)^2}\right]. \quad (8)$$

The beam propagates with velocity $\boldsymbol{\beta}_{\rm b}c = (1 - 1/\Gamma_{\rm b}^2)^{1/2}\,\boldsymbol{x}$; the relativistic beam plasma frequency (in the upstream frame) is given by

$$\omega_{\rm pb} \equiv \left(\frac{4\pi n_{\rm b|u} e^2}{\Gamma_{\rm b} m_{\rm p}}\right)^{1/2}, \quad (9)$$

recalling $\Gamma_{\rm b} \simeq \Gamma_{\rm sh}^2$. One can solve the dispersion relation, including the beam response, to first order in $\chi^{\rm b}$ since its contribution is of order:

$$\left(\frac{\omega_{\rm pb}}{\omega_{\rm pe}}\right)^2 = \frac{m_{\rm e}}{m_{\rm p}}\xi_{\rm cr} \ll 1. \quad (10)$$

### 3.1 Weibel/filamentation instability

Consider now a mode with $k_y = 0$, but $k_x \neq 0$, $k_z \neq 0$. The dispersion relation, including the beam response can be written as follows, to first order in $\chi^{\rm b}_{ij}$,

$$\left(\omega^2 - \omega_{\rm p}^2 - k^2c^2 - \chi^{\rm b}_{yy}\omega^2\right) \times \left[\left(\omega^2 - \omega_{\rm p}^2 - k_z^2c^2 + \chi^{\rm b}_{xx}\right)\left(\omega^2 - \omega_{\rm p}^2 - k_x^2c^2 + \chi^{\rm b}_{zz}\right) - \left(k_xk_zc^2 + \chi^{\rm b}_{xz}\omega^2\right)^2\right] = 0, \quad (11)$$

with $\omega_{\rm p}^2 \equiv \omega_{\rm pi}^2 + \omega_{\rm pe}^2$. In the limit $k_x \to 0$, one recovers the filamentation (Weibel like) instability by developing the above dispersion relation to first order in $\chi^{\rm b}$, with

$$\omega^2 = -\omega^2_{\rm pb}\frac{k^2c^2}{\omega_{\rm p}^2 + k^2c^2}. \quad (12)$$

It saturates at a growth rate $\mathcal{I}(\omega_{\rm We.}) \simeq \omega_{\rm pb}$ in the limit $kc \gg \omega_{\rm p}$.

### 3.2 Čerenkov resonance with oblique electrostatic modes

In the other limit $k_z \to 0$, one can simplify the dispersion relation for electrostatic modes down to

$$\omega^2 - \omega_{\rm p}^2 + \chi^{\rm b}_{xx}\omega^2 \simeq 0. \quad (13)$$

Then, the two stream instability resonance condition between the Langmuir modes and the beam reads

$$\omega = \omega_{\rm p}(1+\delta) = \beta_{\rm b}k_xc(1+\delta), \quad (14)$$

with by assumption $|\delta| \ll 1$. After insertion into equation (13), this yields

$$\delta^3 = \frac{\omega^2_{\rm pb}}{2\Gamma_{\rm b}^2\omega_{\rm p}^2}, \quad (15)$$

hence a growth rate

$$\mathcal{I}(\omega) \simeq \frac{\sqrt{3}}{2^{4/3}}\left(\frac{\omega^2_{\rm pb}\omega_{\rm p}}{\Gamma_{\rm b}^2}\right)^{1/3}. \quad (16)$$

One should note that the Čerenkov resonance can only take place with plasma modes with phase velocity smaller than $c$ [refraction index $kc/\omega(k) > 1$], hence transverse modes are excluded in this respect.

The oblique mode, with $k_z \neq 0$ and a resonance as above yields a growth rate that is larger by a factor of $\Gamma_{\rm b}^{2/3}$ than the two stream rate given in equation (16) for $k_z = 0$ (Bret et al. 2004, 2005a,b). This can be understood as follows. The instability arises from the $xx$ component of the beam susceptibility tensor, which dominates over the other components at the resonance (see equation 8), and which reads

$$\chi^{\rm b}_{xx} = -\frac{\omega^2_{\rm pb}}{\omega^2}\frac{\omega^2/\Gamma_{\rm b}^2 + \beta_{\rm b}^2k_z^2c^2}{(\omega - \beta_{\rm b}k_xc)^2}. \quad (17)$$

This component is suppressed by $1/\Gamma_{\rm b}^2$ when $k_z = 0$, which explains the factor appearing in the right-hand side of equation (16). For $k_z \neq 0$, however, the algebra is more cumbersome. Nevertheless, proceeding as above, with the resonance condition equation (14), one obtains in the limit $\delta \ll 1$ and $\beta_{\rm b} \simeq 1$,

$$\delta^3 \simeq \frac{\omega^2_{pb}}{\omega_{\rm p}^2}\frac{k_z^2}{2k^2}. \quad (18)$$

In the limit $k_z \gg k_x \simeq \omega_{\rm p}/c$, one recovers the growth rate of the oblique mode,

$$\mathcal{I}(\omega) \simeq \frac{\sqrt{3}}{2^{4/3}}\left(\omega^2_{\rm pb}\omega_{\rm p}\right)^{1/3}. \quad (19)$$

This mode obviously grows faster than the previous two.

Obviously, the mode is quasi-longitudinal, since resonance takes place with the electrostatic modes. However, it also comprises a small electromagnetic component, $|B_y|/|E_z| \approx 2|\delta|$, as can be seen by solving for the eigenmode, using the full dispersion relation including the beam contribution.

## 4 INSTABILITIES IN THE PRESENCE OF A MEAN FIELD

As before, we look for an instability of the upstream plasma waves, triggered by the beam of accelerated (and shock reflected) particles. At non-relativistic shocks, one usually considers an interaction at the Larmor resonance. However, this cannot be relevant in the ultra-relativistic case, because the interaction must develop on a distance scale $\lesssim \ell_{\rm F}$ which is itself much shorter than the Larmor radius. The particular case of a relativistic parallel shock wave will be briefly discussed thereafter. Note finally that for the frequently valid condition $\beta_{\rm A}\,\Gamma_{\rm sh}\sin\theta_B \ll 1$, the precursor has a length much larger than the minimum scale for magnetohydrodynamics (MHD) description ($\ell_{\rm MHD}/\ell_{\rm F|u} = \beta_{\rm A}\Gamma_{\rm sh}\sin\theta_B$), which justifies the resonance between the beam and the MHD modes.

### 4.1 Oblique magnetic field

In order to excite fast waves of frequency higher than the Larmor frequency, we consider again the Čerenkov resonance between the non-magnetized beam and the magnetized plasma waves: $\omega - \boldsymbol{k}\cdot\boldsymbol{v}_{\rm b} = 0$. Let us recall that for a ultra-relativistic beam, the velocity distribution is strongly peaked at $v_{\rm b} \sim c$, even if the dispersion in Lorentz factor of the beam is significant. We also discuss the possibility of generating the magnetic field through a (non-resonant) Weibel (filamentation) instability with $k_x = 0$.

#### 4.1.1 Weibel – filamentation instability

This instability taking place in the shock transition layer between the unshocked plasma and the shocked plasma has been discussed in detail in the waterbag approximation for an unmagnetized plasma (Medvedev & Loeb 1999; Wiersma & Achterberg 2004; Lyubarsky & Eichler 2006; Achterberg & Wiersma 2007; Achterberg et al. 2007). As we now argue, the Weibel instability can also proceed in the regime of unmagnetized proton – magnetized plasma electrons at smaller frequencies, corresponding to the range $\omega_{\rm ci} \ll \omega \ll \omega_{\rm ce}$ (see also Achterberg & Wiersma 2007). Again, we should stress that we consider a pure ion beam (reflected and accelerated particles), whereas most above studies consider two neutral interpenetrating plasmas.

To simplify the algebra, we write down the dispersion relation in a frame in which the $(\boldsymbol{x}, \boldsymbol{z})$ plane has been rotated in such a way as to align $\boldsymbol{B}$ with the third axis, denoted $\boldsymbol{z}_B$; $\boldsymbol{y}$ remains the second axis $\boldsymbol{y}_B$. To simplify further a cumbersome algebra, we consider a wavenumber $\boldsymbol{k} \parallel \boldsymbol{y}_B$, perpendicular to both the beam motion and the magnetic field. The plasma dielectric tensor is written in this $B$ frame as

$$\Lambda_{ij|B} = \begin{pmatrix} \varepsilon_1 - \eta^2 & i\varepsilon_2 & 0 \\ -i\varepsilon_2 & \varepsilon_1 & 0 \\ 0 & 0 & \varepsilon_\parallel - \eta^2 \end{pmatrix}, \tag{20}$$

with the following usual definitions (for $\omega_{\rm ci} \ll \omega \ll \omega_{\rm ce}$):

$$\varepsilon_1 \simeq 1 - \frac{\omega_{\rm pi}^2}{\omega^2} + \frac{\omega_{\rm pe}^2}{\omega_{\rm ce}^2}, \quad \varepsilon_2 \simeq \frac{\omega_{\rm pe}^2}{\omega\omega_{\rm ce}}, \quad \varepsilon_\parallel \simeq 1 - \frac{\omega_{\rm p}^2}{\omega^2} \tag{21}$$

and $\eta \equiv kc/\omega$. One needs to rotate the beam susceptibility tensor to this $B$ frame. The quantity of interest will turn out to be the 3–3 component $\chi^{\rm b}_{z_B z_B} = \cos^2\theta_B \chi^{\rm b}_{xx} + \sin^2\theta_B \chi^{\rm b}_{zz}$. To first order in $\chi^{\rm b}$, the dispersion relation indeed has the solution:

$$\varepsilon_\parallel - \eta^2 + \cos^2\theta_B \chi^{\rm b}_{xx} + \sin^2\theta_B \chi^{\rm b}_{zz} = 0. \tag{22}$$

Given the dependence of $\chi^{\rm b}_{xx}$ on $\omega$, this is a quartic equation which admits the solution leading to the Weibel (filamentation) instability,

$$\omega^2 \simeq -\omega_{\rm pb}^2 \cos^2\theta_B \frac{k^2c^2}{\omega_{\rm p}^2 + k^2c^2}. \tag{23}$$

As in the unmagnetized case, it saturates at a growth rate $\simeq \omega_{\rm pb} \cos\theta_B$ (up to the angular dependence on $B$). Note that in the limit $\cos\theta_B \to 0$, this instability does not disappear. In order to see this, one has to consider the other branch of the dispersion relation, for $\cos\theta_B = 0$, $\boldsymbol{k} = k_z\,\boldsymbol{z}$,

$$\left(\epsilon_1 - \eta^2 + \chi^{\rm b}_{xx}\right)\left(\epsilon_1 - \eta^2 + \chi^{\rm b}_{yy}\right) - \epsilon_2^2 = 0. \tag{24}$$

One of the roots corresponds to the Whistler mode and the other to the Weibel unstable mode with $\omega^2 \simeq -\omega_{\rm pb}^2$.

The above thus shows that fast waves can be excited by the relativistic stream in the intermediate range between MHD and electron dynamics, i.e. with unmagnetized plasma ions but magnetized electrons. The typical length scale of these waves for which maximal growth occurs is obviously the electron inertial scale $\delta_{\rm e} \equiv c/\omega_{\rm p}$ as before.

#### 4.1.2 Čerenkov resonance with longitudinal modes

The previous discussion of the Čerenkov instability with electrostatic modes can be generalized to the magnetized plasma limit by considering those modes with $\boldsymbol{k} \parallel \boldsymbol{B}$, which do not feel the magnetic field (see Lyubarsky 2002 for a discussion of this instability in the case of pulsar magnetospheres). Rewriting the above plasma dielectric tensor for a wavenumber parallel to the magnetic field, it is straightforward to see that the dispersion relation admits the longitudinal branch given by

$$\varepsilon_\parallel + \cos^2\theta_B \chi^{\rm b}_{xx} + \sin^2\theta_B \chi^{\rm b}_{zz} = 0. \tag{25}$$

In order to avoid confusion, it may be useful to stress that the previous *oblique* denomination refers to the angle between the wavenumber and the beam direction, while the present term *longitudinal* here refers to the parallel nature of $\boldsymbol{k}$ and $\boldsymbol{B}$. At the Čerenkov resonance $\omega = \omega_{\rm p}(1+\delta) = \beta_{\rm b} k_x c(1+\delta)$, with $|\delta| \ll 1$, one has $|\chi^{\rm b}_{xx}| \gg |\chi^{\rm b}_{zz}|$, therefore one can obtain the following approximate solution for the growth rate

$$\mathcal{I}(\omega) \simeq \frac{\sqrt{3}}{2^{4/3}} \left[\omega_{\rm pb}^2 \omega_{\rm p} \cos^2\theta_B \left(\frac{1}{\Gamma_{\rm b}^2} + \frac{k^2c^2\sin^2\theta_B}{\omega_{\rm p}^2}\right)\right]^{1/3}. \tag{26}$$

Recalling that $k_x = k\cos\theta_B = \omega_{\rm p}/c$, and that $\Gamma_{\rm b}^2 = \Gamma_{\rm sh}^4$, one can neglect in all generality the first term in the parenthesis, so that $\mathcal{I}(\omega) \simeq (\omega_{\rm pb}^2 \omega_{\rm p} \sin^2\theta_B)^{1/3}$.

#### 4.1.3 Resonant instability with Alfvén modes

Turning now to resonant instabilities with Alfvén waves, we consider a wave vector in the $(\boldsymbol{x}, \boldsymbol{z})$ plane. The resonance condition for Alfvén modes reads: $\beta_{\rm b} k_x \simeq \beta_{\rm A} k \cos\theta_k$, where $\theta_k$ represents the angle between the wavenumber and the magnetic field direction. Since $\beta_{\rm A} < 1$, this implies $k_x \ll k$, therefore the wavenumber is mostly aligned along $\boldsymbol{z}$ and $\theta_k \simeq \pi/2 - \theta_B$.

The plasma dielectric tensor now reads (we omitted negligible contributions in $\sin^2\theta_k$)

$$\Lambda_{ij|B} = \begin{pmatrix} \varepsilon_1 - \eta^2\cos^2\theta_k & i\varepsilon_2 & \eta\cos\theta_k\sin\theta_k \\ -i\varepsilon_2 & \varepsilon_1 - \eta^2 & 0 \\ \eta\cos\theta_k\sin\theta_k & 0 & \varepsilon_\parallel - \eta^2\sin^2\theta_k \end{pmatrix}, \tag{27}$$

with $(\omega \ll \omega_{\rm ci})$

$$\varepsilon_1 \simeq \frac{1}{\beta_A^2}, \ \varepsilon_2 \simeq 0, \ \varepsilon_\parallel \simeq -\frac{\omega_{\rm p}^2}{\omega^2}. \tag{28}$$

The beam susceptibility can be approximated accurately by neglecting all components in front of $\chi^{\rm b}_{xx}$, which dominates at the resonance, as explained above. The relevant components then are

$$\begin{aligned} &\chi^{\rm b}_{x_B x_B} \simeq \sin^2\theta_B \chi^{\rm b}_{xx}, \ \chi^{\rm b}_{z_B z_B} \simeq \cos^2\theta_B \chi^{\rm b}_{xx}, \\ &\chi^{\rm b}_{x_B z_B} = \chi^{\rm b}_{z_B x_B} \simeq \sin\theta_B \cos\theta_B \chi^{\rm b}_{xx}. \end{aligned} \tag{29}$$

The dispersion relation then takes the form:

$$\begin{aligned} &\left(\frac{\omega^2}{\beta_A^2} - k^2c^2\cos^2\theta_k\right)\left(\omega_{\rm p}^2 + k^2c^2\sin^2\theta_k\right) \\ &+ k^4c^4\sin^2\theta_k\cos^2\theta_k - \omega^4 A_{xx}\chi^{\rm b}_{xx} = 0, \end{aligned} \tag{30}$$

where $A_{xx} \simeq -\sin^2\theta_B \omega_{\rm p}^2/\omega^2$ in the limit $k\delta_{\rm e} \ll 1$. Writing down the resonance condition $\omega = \beta_A k\cos\theta_k c\,(1+\delta) = \beta_{\rm b} k_x c\,(1+\delta)$, with $|\delta| \ll 1$ as before, one obtains the growth rate

$$\mathcal{I}(\omega) \simeq \frac{\sqrt{3}}{2^{4/3}} \left(\omega_{\rm pb}^2 \beta_{\rm A} kc\cos\theta_k\right)^{1/3}, \tag{31}$$

where we approximated $k_z \simeq k$; recall furthermore that $\cos\theta_k \simeq \sin\theta_B$. This instability disappears in the limit of a parallel shock wave as one can no longer satisfy the Čerenkov resonance condition.

One should stress that the above perturbative treatment remains valid as long as the condition $|\delta| \ll 1$, which amounts to $\xi_{\rm cr} \ll \beta_{\rm A}^2$ at

maximum wave growth rate ($kc = \omega_{\rm ci}$). Therefore, Alfvén growth is limited to strongly magnetized shock waves only.

In the continuity of right Alfvén waves (the left modes being absorbed at the ion-cyclotron resonance), there are Whistler waves for quasi-parallel propagation (with respect to the mean field), that are electromagnetic waves with a dominant magnetic component. For quasi-perpendicular propagation, there are the ionic extraordinary modes, which have frequencies between the ion-cyclotron frequency and the low-hybrid frequency (obtained for large refraction index) and which are mostly electrostatic with a weaker electromagnetic component. For scattering purpose, the whistler waves are the most interesting in this intermediate range; they are actually excited in the foot of non-relativistic collisionless shocks in space plasmas. But for pre-heating purposes, the extraordinary ionic modes are more interesting (they are actually used for additional heating in tokamaks). Let us now discuss these in turn.

#### *4.1.4 Resonant instability with Whistler waves*

We proceed as before, using the plasma dielectric tensor equation (27) in the range $\omega_{\rm ci} \ll \omega \ll \omega_{\rm ce}$ with the components given in equation (21). The Whistler branch of the dispersion relation reads, to first order in the beam response $\chi^{\rm b}$ approximated by equation (29),

$$\left(\epsilon_1 - \eta^2 \cos^2\theta_k + \chi^{\rm b}_{xx} \sin^2\theta_B\right)\left(\epsilon_1 - \eta^2\right) - \epsilon_2^2 \,=\, 0. \tag{32}$$

When the beam response is absent, one recovers the dispersion relation for oblique Whistler waves,

$$\omega^2_{\rm Wh.} \,\simeq\, \frac{\omega^2_{\rm ce}}{\omega^4_{\rm pe}} k^4 c^4 \cos^2\theta_k. \tag{33}$$

Introducing the resonance $\omega = \omega_{\rm Wh.}(1+\delta) = \beta_{\rm b}\, k_x c(1+\delta)$, with $|\delta| \ll 1$, we obtain the growth rate

$$\mathcal{I}(\omega) \,\simeq\, \frac{\sqrt{3}}{2^{4/3}} \left(\omega^2_{\rm pb}\omega_{\rm Wh.}\right)^{1/3}. \tag{34}$$

In the latter equation, we again approximated $k_z \simeq k$, since the resonance condition implies $k_x \ll k$ (therefore $\cos\theta_k \simeq \sin\theta_B$). The instability disappears in the limit of a parallel shock wave as well, because the resonance condition cannot be satisfied. Maximum growth occurs here as well for $k \simeq c/\omega_{\rm pe} \simeq c/\omega_{\rm p}$, i.e. at the electron inertial scale $\delta_{\rm e}$, however, the excitation range extends to the proton inertial scale $\delta_{\rm i}$ where it matches with the Alfvén wave instability.

As before, the perturbative treatment remains valid as long as $|\delta| \ll 1$, which amounts to $\xi_{\rm cr} \ll (m_{\rm p}/m_{\rm e})^2 \beta_{\rm A}^2$. This condition is more easily satisfied that the corresponding one for amplification of Alfvén waves. It will be discussed in more detail in Section 5.

#### *4.1.5 Resonant instability with extraordinary modes*

At MHD scales, the extraordinary ionic modes (that propagate with wave vectors almost perpendicular to the magnetic field) assimilate to magneto-sonic modes. These modes have been shown to be unstable when there is a net electric charge carried by the cosmic rays (Pelletier et al. 2009). The obtained growth rates are increasing with wave numbers indicating an instability that reaches its maximum growth at scales shorter than the MHD range. Let us therefore discuss how this instability extends to sub-MHD scales.

Let us first discuss the ionic (lower hybrid) branch, $\omega < \omega_{\rm lh}$, with $\omega_{\rm lh} \equiv \sqrt{\omega_{\rm ci}\omega_{\rm ce}}$. In the following, we assume for simplicity $\omega_{\rm ce} \ll \omega_{\rm pe}$, i.e. a weakly magnetized plasma. In the $\boldsymbol{B}$ frame, in which $\boldsymbol{B}$ is along $\boldsymbol{z}_B$ and the beam propagates in the $(\boldsymbol{x}, \boldsymbol{z})$ plane, take $\boldsymbol{k} \parallel \boldsymbol{y}_B$, with a small component $k_{x_B}$, i.e. in the $(x, z)$ plane but perpendicular to $B$. The dispersion relation to zeroth order in $\chi^{\rm b}$ reads

$$\eta^2 \,=\, \frac{\epsilon_1^2 - \epsilon_2^2}{\epsilon_1}. \tag{35}$$

with (since $\omega < \omega_{\rm lh} \ll \omega_{\rm ce}$)

$$\frac{\epsilon_1^2 - \epsilon_2^2}{\epsilon_1} \,\simeq\, \frac{\omega^2_{\rm ce}}{\omega^2_{\rm ci}\omega^2_{\rm pe}} \frac{\omega^2\omega^2_{\rm ci} - \left(\omega^2_{\rm ci} + \omega^2_{\rm pi}\right)^2}{\omega^2 - \omega^2_{\rm lh}}, \tag{36}$$

hence

$$\begin{aligned} \frac{\epsilon_1^2 - \epsilon_2^2}{\epsilon_1} \,&\simeq\, \frac{\omega^2_{\rm pi}}{\omega^2_{\rm ci}} \quad (\omega \,\ll\, \omega_{\rm ci}), \\ \frac{\epsilon_1^2 - \epsilon_2^2}{\epsilon_1} \,&\simeq\, \frac{\omega^2_{\rm pe}}{\omega^2_{\rm lh} - \omega^2} \quad (\omega_{\rm ci} \,\ll\, \omega \,\ll\, \omega_{\rm lh}). \end{aligned} \tag{37}$$

At $\omega \ll \omega_{\rm ci}$, this gives the fast magnetosonic branch with $\omega_{\rm H} \simeq \beta_{\rm A} kc$, while at $\omega_{\rm ci} \,\ll\, \omega \,\ll\, \omega_{\rm lh}, \omega_{\rm H} \,\sim\, \omega_{\rm lh} kc/\sqrt{k^2c^2 + \omega^2_{\rm pe}}$. We define

$$\mathcal{D}(k, \omega) \,\equiv\, \frac{\epsilon_1^2 - \epsilon_2^2}{\epsilon_1} - \eta^2. \tag{38}$$

so that

$$\begin{aligned} \omega^2 \frac{\partial}{\partial\omega^2}\mathcal{D}(k,\omega) \,&\simeq\, \eta^2 \quad (\omega \,\ll\, \omega_{\rm ci}), \\ \omega^2 \frac{\partial}{\partial\omega^2}\mathcal{D}(k,\omega) \,&\simeq\, \eta^2 \frac{\omega^2_{\rm lh}}{\omega^2_{\rm lh} - \omega^2} \quad (\omega_{\rm ci} \,\ll\, \omega \,\ll\, \omega_{\rm lh}). \end{aligned} \tag{39}$$

Including the beam response, the dispersion relation becomes

$$\epsilon_1^2 - \epsilon_2^2 - \epsilon_1\eta^2 + \left(\epsilon_1 - \eta^2_{x_B}\right)\sin^2\theta_B \chi^{\rm b}_{xx} \,=\, 0. \tag{40}$$

We neglect the term $\eta^2_{x_B} \,\ll\, \eta^2$ in front of $\epsilon_1 \sim 1/\beta^2_{\rm A}$ (at $\omega \ll \omega_{\rm ci}$). At the resonance $\omega = \omega_{\rm H}(1+\delta)$, with $\omega_{\rm H}$ the solution of $\mathcal{D}(k, \omega_{\rm H}) \,=\, 0$, one finds

$$\delta^3 \,\simeq\, \frac{1}{2}\frac{\omega^2_{\rm pb}\sin^2\theta_B}{\omega^2_{\rm H}} \left[\omega^2 \frac{\partial}{\partial\omega^2}\mathcal{D}(k,\omega)\right]^{-1} \frac{k_y^2 c^2}{\omega^2_{\rm H}}. \tag{41}$$

The growth rate for Čerenkov resonance with the lower hybrid extraordinary mode thus reads

$$\begin{aligned} \mathcal{I}(\omega_{\rm LX}) \,&\simeq\, \frac{\sqrt{3}}{2^{4/3}} \left(\omega^2_{\rm pb}\sin^2\theta_B \frac{k_y^2}{k^2}\beta_{\rm A} kc\right)^{1/3} \quad (\omega \,\ll\, \omega_{\rm ci}), \\ \mathcal{I}(\omega_{\rm LX}) \,&\simeq\, \frac{\sqrt{3}}{2^{4/3}} \left[\omega^2_{\rm pb}\sin^2\theta_B \frac{k_y^2}{k^2} \frac{\omega_{\rm lh}\omega^2_{\rm pe} kc}{\left(k^2c^2 + \omega^2_{\rm pe}\right)^{3/2}}\right]^{1/3} \\ &\qquad (\omega_{\rm ci} \,\ll\, \omega \,\ll\, \omega_{\rm lh}). \end{aligned} \tag{42}$$

In the limit of magnetosonic modes, $\omega \ll \omega_{\rm ci}$, one recovers the same growth rate as for Alfvén waves; note that $\beta_{\rm A} kc \,\ll \omega_{\rm ci}$ implies $k \ll \omega_{\rm pi}/c$. At smaller scales, one finds that the growth rate reaches its maximum at $k \simeq \omega_{\rm pe}/c$ with $\mathcal{I}(\omega_{\rm LX}) \,\sim\, (\omega^2_{\rm pb}\sin^2\theta_B\omega_{\rm lh})^{1/3}$. We can expect this instability to provide efficient heating of the protons in the foot.

Turning to the electronic (upper hybrid) modes, around $\omega \sim \omega_{\rm pe}$, one obtains

$$\frac{\epsilon_1^2 - \epsilon_2^2}{\epsilon_1} \,\simeq\, \frac{(\omega^2 - \omega_x^2)(\omega^2 - \omega_z^2)}{\omega^2_{\rm pe}(\omega^2 - \omega^2_{\rm uh})}, \tag{43}$$

with $\omega_x \simeq \omega_{\rm pe} - \omega_{\rm ce}/2, \omega_z \simeq \omega_{\rm pe} + \omega_{\rm ce}/2$ and $\omega_{\rm uh} \,\equiv\, \left(\omega_p^2 + \omega^2_{\rm ce}\right)^{1/2}$. The dispersion relation takes the same form $\mathcal{D}(k, \omega) = 0$, but now

$$\frac{\partial}{\partial\omega^2}\mathcal{D}(k,\omega) \,\simeq\, \eta^2 \left(\frac{\omega^2}{\omega^2 - \omega_x^2} + \frac{\omega^2}{\omega^2 - \omega_z^2} - \frac{\omega^2}{\omega^2 - \omega^2_{\rm uh}} + 1\right). \tag{44}$$

The growth rate can be written in the same algebraic form as (41). It vanishes in both limits $\omega \to \omega_x$ and $\omega \to \omega_z$, while for $\omega \simeq \omega_{pe}$, giving $\eta \simeq 1$, one obtains

$$\mathcal{I}(\omega_{UX}) \simeq \frac{\sqrt{3}}{2^{4/3}} \left( \omega_{pb}^2 \sin^2\theta_B \omega_{pe} \frac{\omega_{ce}^2}{\omega_{pe}^2} \frac{k_y^2}{k^2} \right)^{1/3}. \quad (45)$$

It vanishes in the limit $\omega_{ce}/\omega_{pe} \to 0$, in which limit the electronic extraordinary branch actually disappears.

Being electrostatic in nature, these waves participate mostly to the heating process in the shock foot or precursor. However, their scattering efficiency is comparable to the magnetic perturbations as will be seen further on.

### 4.2 The particular case of a parallel magnetic field

When the magnetic field is almost parallel, i.e. $\theta_B < 1/\Gamma_{sh}$, the relativistic Bell non-resonant instability (Bell 2004, 2005) can develop (e.g. Milosavljević & Nakar 2006; Reville et al. 2006). This instability is triggered by the charge current carried by the cosmic rays in the precursor, which induces a return current in the plasma, thereby destabilizing non-resonant waves of wavelength shorter than the typical Larmor radius, the cosmic rays being unresponsive to the excitation of the waves. The growth rate of this instability in the upstream frame is (Reville et al. 2006)

$$\mathcal{I}(\omega_{Bell}) \simeq \frac{\beta_b n_{b|u}}{n_u} \omega_{pi}, \quad (46)$$

and growth is maximal at the scale $k_c \simeq \mathcal{I}(\omega_{Bell})/(\beta_A c)$.

One can then verify that, under quite general assumptions, this growth rate is larger than the growth rate of the Weibel instability, since the ratio of these two is given by

$$\frac{\mathcal{I}(\omega_{Bell})}{\mathcal{I}(\omega_{We.})} \simeq \Gamma_{sh}^2 \xi_{cr}^{1/2}. \quad (47)$$

One must emphasize, however, that the Bell instability is quenched when the growth rate exceeds the ion cyclotron frequency see Couch, Milosavljevic & Nakar (2008), Riquelme & Spitkovsky (2009) and Ohira et al. (2009). This limitation will be made clear in Section 5.2.

## 5 LIMITATIONS OF THE INSTABILITIES

Using the growth rates derived previously, we can now delimit the conditions under which the various instabilities become effective, and which one dominates. We then discuss the limit between unmagnetized and magnetized shock waves, from the point of view of these upstream instabilities.

### 5.1 Superluminal shock waves

In this section, we discuss the generic case of relativistic superluminal shock waves, taking $\sin^2\theta_B \sim 1$. Unless otherwise noted, we assume an $e-p$ plasma; we will discuss how the results are modified in the limit of a pair plasma at the end of this discussion. The more particular case of relativistic parallel shock waves is treated further below.

We start by introducing the two parameters $X$ and $Y$ defined as follows:

$$X \equiv \Gamma_{sh} \frac{m_e}{m_p},$$

$$Y \equiv \Gamma_{sh}^4 \frac{B_{u|u}^2}{4\pi n_{b|u} m_p c^2} = \Gamma_{sh}^2 \sigma_u \xi_{cr}^{-1}. \quad (48)$$

The upstream magnetization parameter $\sigma_u$ also corresponds to the Alfvén velocity squared of the upstream plasma (in units of $c^2$). If the field is fully perpendicular, the shock crossing conditions imply $B_{d|d,\perp} \simeq B_{u|u,\perp}\Gamma_{sh}\sqrt{8}$, and for the enthalpy $h_{d|d} \simeq (8/3)\Gamma_{sh}^2 h_{u|u}$ (for a cold upstream plasma, see Blandford & McKee 1976), so that $\sigma_d \simeq 3\sigma_u \sin^2\theta_B$. If the magnetic field is mostly parallel, meaning $\sin\theta_B \leq 1/\Gamma_{sh}$, then $\sigma_d \sim (3/8)\Gamma_{sh}^{-2}\sigma_u$.

Let us first compare the growth rates of the instabilities obtained in the magnetized case; the unmagnetized case (in particular the oblique mode) will be discussed thereafter. We carry out this comparison at the wavenumber where the growth rates reach their maximum, namely $k \sim \omega_{pe}/c$. The ratio of the Weibel to Whistler instability growth rates is given by

$$\frac{\mathcal{I}(\omega_{We.})}{\mathcal{I}(\omega_{Wh.})} = \left(\frac{X}{Y}\right)^{1/6}, \quad (49)$$

hence the Weibel instability will dominate over the Whistler Čerenkov resonant instability whenever $Y \ll X$. The fastest mode, however, corresponds to the Čerenkov resonance with the longitudinal modes along the magnetic field, since the ratio of the growth rates of this mode to the Weibel mode is $(m_p/m_e)^{1/6}\,\xi_{cr}^{-1/6}$, which is always greater than one.

Since the Čerenkov resonant instabilities for the Whistler and Alfvén waves scale in a similar way with the eigenfrequencies of the resonant plasma modes, it is straightforward to see that Whistler waves will always grow faster than the Alfvén waves.

Concerning the extraordinary modes, one finds that $\mathcal{I}(\omega_{Wh.})/\mathcal{I}(\omega_{LX}) \sim (m_p/m_e)^{1/6}$ on the ionic (lower hybrid) branch, while $\mathcal{I}(\omega_{Wh.})/\mathcal{I}(\omega_{UX}) \sim (\omega_{pe}/\omega_{ce})^{1/3}$ on the electronic (upper hybrid) branch. Therefore, the growth of these modes is always subdominant with respect to that of Whistler and Weibel modes. Since the growth rates of the Alfvén and extraordinary modes are always smaller than that of the Whistler modes, we discard the former in the following.

Additional constraints can be obtained as follows. First of all, the above derivation of the instabilities has assumed the beam to be unmagnetized, i.e. that the growth time be much shorter than the Larmor time of the beam particles. This condition is always easily satisfied, since it reads: $Y \ll \Gamma_{sh}^6$ for the Weibel instability, $Y \ll \Gamma_{sh}^6 \xi_{cr}^{-1/3}\,(m_e/m_p)^{-1/3}$ for the longitudinal mode and $Y \ll \Gamma_{sh}^8 m_p/m_e$ for the Whistler Čerenkov resonant mode. One can explicit the dependence of $Y$ on the shock parameters in order to verify this; for the Weibel instability, the condition amounts to $\xi_{cr} \gg \Gamma_{sh}^{-4}\,\sigma_u$, which is indeed easily verified at large Lorentz factors.

Concerning the Čerenkov resonant modes, one must also require that $|\delta| < 1$ in order for the perturbative treatment to be apply. In the case of longitudinal modes, this is automatically satisfied since $\omega_{pb} < \omega_p$. However, for Whistler modes of smaller eigenfrequency, this implies a non-trivial constraint $\omega_{pb} < \omega_{Wh.}$ which can be translated into $Y \gg X^2$ for $\omega_{Wh.} = \omega_{ce}$.

Further bounds can be obtained by requiring that the background protons are non-magnetized in the case of the Weibel instability, which requires $\mathcal{I}(\omega) \gg \omega_{ci}$. This condition is, however, superseded by the requirement that the growth can occur on the precursor length scale, since $\ell_F/c \sim (\Gamma_{sh}\,\omega_{ci})^{-1}$ (see equation 5). At this stage, it is important to point out a fundamental difference between the Čerenkov resonant instabilities and the Weibel/filamentation instabilities. The former have, by definition of the resonance, a phase velocity along the shock normal which, to zeroth order in $|\delta|$ exceeds the shock velocity, while the latter have vanishing phase velocity along $\boldsymbol{x}$. Therefore, the time-scale available for the growth of these non-resonant waves is the crossing time of the precursor: they are

sourced at a typical distance $\ell_{\rm F}$ away from the shock, then advected downstream on this time-scale. Regarding the resonant modes, their phase velocity along $\boldsymbol{x}$ is $\beta_{\phi,x} = \beta_{\rm b}(1+\delta_{\rm R})$, with $\delta_{\rm R} = \mathcal{R}(\delta)$. Since $\delta_{\rm R} < 0$ for the resonant modes, one must consider three possible cases: (i) $\beta_{\phi,x} < \beta_{\rm sh}$, in which case the mode is advected away on a time-scale $\ell_{\rm F}/c$ as for the non-resonant modes; (ii) $\beta_{\phi,x} > \beta_{\rm sh}$, in which case the mode propagates forward, but exits the precursor (where it is sourced) on a similar time-scale and (iii) $\beta_{\phi,x} \simeq \beta_{\rm sh}$, in which case the mode can be excited on a time-scale $\simeq c^{-1}\ell_{\rm F}/(\beta_{\rm sh} - \beta_{\phi,x})$ and where the divergence corresponds to the situation of a mode surfing on the shock precursor. However, condition (i) appears to be the most likely, as least in the ultra-relativistic limit, for it amounts to $2\Gamma_{\rm sh}^2|\delta_{\rm R}| \gg 1$. Indeed, all resonant instabilities have a growth rate $\sim(\omega_{\rm pb}^2\omega)^{1/3}$ where $\omega$ is the eigenfrequency of the resonant mode [an exception is the upper hybrid mode for which the growth rate is smaller by $(\omega_{\rm ce}/\omega_{\rm pe})^{2/3}$, in which case the following condition is even stronger], therefore the condition $2\Gamma_{\rm sh}^2|\delta_{\rm R}| \gg 1$ can be rewritten as $\omega/\omega_{\rm pe} \ll 7\,(\Gamma_{\rm sh}/10)^3(\xi_{\rm cr}/0.1)^{1/2}$, which is generically satisfied. This means that the phase velocity of the resonant modes, when corrected by the effect of the beam becomes smaller than the shock front velocity, so that these modes are advected on a time-scale $\sim\ell_{\rm F}/c$ and transmitted downstream, after all. For the purpose of magnetic field amplification downstream and particle acceleration, this is certainly noteworthy, as such true plasma eigenmodes (Whistler, Alfvén, extraordinary and electrostatic longitudinal or oblique modes) can be expected to have a longer lifetime than the Weibel modes.

The modes thus grow on the precursor crossing time-scale if $\mathcal{I}(\omega)\,\ell_{\rm F}/c \gg 1$, which can be recast as $Y \ll 1$ for the Weibel instability, $Y \ll \xi_{\rm cr}^{-1/3}\,(m_{\rm e}/m_{\rm p})^{-1/3}$ and $XY \ll 1$ for the Čerenkov resonant Whistler mode. Henceforth, we use the parameter $G \equiv (\omega_{\rm pb}/\omega_{\rm p})^{-2/3} = \xi_{\rm cr}^{-1/3}\,(m_{\rm e}/m_{\rm p})^{-1/3} > 1$.

In short, we find that the various instabilities discussed here are more likely quenched by advection rather than by saturation. In Section 6.1, we provide several concrete estimates for cases of astrophysical interest and it will be found that this limit is indeed quite stringent.

Finally, one must also require that the growth rate of the Čerenkov resonant instabilities does not exceed the proper eigenfrequency of the mode. For the Whistler modes, as discussed at the end of Section 4.1.4, this implies $Y \gg X^2$.

In Section 3, we have also examined the growth rates in the absence of a mean magnetic field, and concluded that the oblique mode of Bret et al. (2004, 2005a,b) was by far the fastest. This instability is very similar to the Čerenkov resonance with the longitudinal modes propagating along the magnetic field and indeed the growth rates only differ by $\sin^{2/3}\theta_B$, see equations (19) and (26). The difference lies in the degree of magnetization of the ambient plasma: while the oblique mode is limited to the unmagnetized limit, the longitudinal mode does not suffer from such constraint; the oblique mode, however, covers a larger fraction of the wavenumber phase space than the longitudinal mode.

With respect to the oblique mode instability, the shock can be described as unmagnetized as long as the background electrons and protons remain unmagnetized on the time-scale of the instability; of course, one must also require that the instability has time to grow on the length scale of the precursor. Note that the latter condition also implies that the beam can be considered as unmagnetized over the instability growth time-scale, which is another necessary condition. For the oblique modes, those conditions amount to

$$\mathcal{I}(\omega_{\rm obl.}) \gg \omega_{\rm ce} \Leftrightarrow Y \ll GX^2, \tag{50}$$

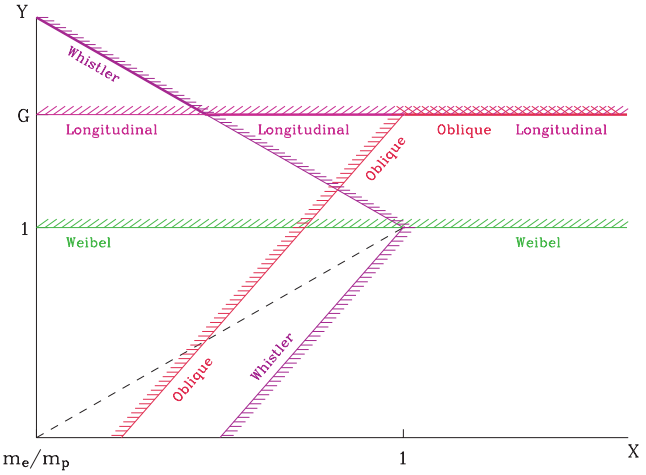


**Figure 1.** Instability diagram for superluminal relativistic shock waves (assuming $\sin^2\theta_B \sim 1$): in abscissa, $X \equiv \Gamma_{\rm sh} m_{\rm e}/m_{\rm p}$, in ordinates $Y \equiv \Gamma_{\rm sh}^4 B_{\rm u}^2/(4\pi n_{\rm b|u} m_{\rm p} c^2)$. The parameter $G = \xi_{\rm cr}^{-1/3}\,(m_{\rm e}/m_{\rm p})^{-1/3} > 1$. The axes are plotted in log–log on arbitrary scale. The main result is summarized by the thick solid line, which indicates the maximum value of $Y(X)$ which allows electromagnetic waves to grow. The other lines indicate the boundaries of the regions of growth of the various instabilities, as indicated. The hierarchy of growth rates, from largest to smallest is as follows: oblique and longitudinal, then Whistler and/or Weibel. The long dashed line separates the regions in which the growth of Whistler or Weibel modes is faster: for values of $Y(X)$ larger than the long dashed line, Whistler modes grow faster. The growth rates of the oblique mode and the longitudinal mode are comparable. Unlike the longitudinal mode, the oblique instability is limited by the assumption of unmagnetization (see main text), but at the same time, it applies to a larger wavenumber phase space. The regions for Alfvén and extraordinary modes are not indicated (see main text).

$$\mathcal{I}(\omega_{\rm obl.}) \gg c/\ell_{\rm F} \Leftrightarrow Y \ll G, \tag{51}$$

with $G = \xi_{\rm cr}^{-1/3}\,(m_{\rm e}/m_{\rm p})^{-1/3} > 1$ as above. Provided the above two conditions are satisfied, the oblique mode dominates over the Weibel and Whistler Čerenkov instability growth rates, just as the longitudinal mode. The Čerenkov resonant instability with Whistler waves dominates over the oblique modes when $X \lesssim G^{-1/3}$ and $GX^2 \lesssim Y \lesssim 1/X$. The Čerenkov resonant instability with Whistler waves dominates over the longitudinal modes when $X \lesssim G^{-1}$ and $G \lesssim Y \lesssim 1/X$. For $X \lesssim G^{-1}$ and $Y \gtrsim X^{-1}$, or for $G^{-1} \lesssim X$ and $Y \gtrsim G$ neither of the above instabilities can grow. For reference, $X \lesssim G^{-1}$ corresponds to $\Gamma_{\rm sh} \lesssim 150\,\xi_{\rm cr}^{1/3}$. The above regions can be summarized in the $X - Y$ plane as in Fig. 1, which delimit the domains in which the various instabilities can grow, and which of these instabilities dominates in each case.

From the above discussion, the case of a pair shock is easily obtained by taking $m_{\rm p}/m_{\rm e} \to 1$, by restricting oneself to the study of the oblique and Weibel modes, and by considering only the right-hand side part of Fig. 1 with $X > 1$, since $X = \Gamma_{\rm sh}$ for a pair shock. One sees that, irrespectively of $\Gamma_{\rm sh}$, the oblique and longitudinal modes can grow if $Y \lesssim \xi_{\rm cr}^{-1/3}$ and the Weibel mode grows on the precursor time-scale if $Y \lesssim 1$.

In this respect, it is instructive to compare the present results with the latest simulations of Sironi & Spitkovsky (2009). These authors find that the growth of instabilities is quenched when the magnetization $\sigma_{\rm u} \gtrsim 0.03$ for a perpendicular (or oblique) pair shock with $\Gamma_{\rm sh} \simeq 20$. This corresponds to $X \simeq 20$ and $Y \simeq 10\xi_{\rm cr}^{-1}\,(\sigma_{\rm u}/0.03)$. Our results indicate that indeed, at this high level of magnetization,

both Weibel and oblique/longitudinal instabilities are quenched by advection. Note that these simulations do not exclude that the instabilities are quenched even at lower magnetizations. Our calculations thus bring to light the following point of interest. One should not infer from the simulations of Sironi & Spitkovsky (2009) that superluminal shock waves cannot lead to magnetic field amplification. This conclusion entirely depends on the level of magnetization. It would therefore be interesting to extend the PIC simulations down to weakly magnetized shocks with $\sigma_{\rm u} \sim 3 \times 10^{-3}\ \xi_{\rm cr}^{2/3}\ (\Gamma_{\rm sh}/20)^{-2}$ in order to probe the limit at which the oblique mode can grow.

### 5.2 Parallel shock waves

In the ultra-relativistic limit, parallel shock waves are non-generic; however, they may lead more easily to particle acceleration than superluminal shock waves (since the argument discussed in (Lemoine et al. 2006) no longer applies) and consequently provide interesting observational signatures. One can extend the above discussion to the case of parallel shock waves as follows.

First of all, the main limitation of the instabilities, that is due to the precursor crossing time-scale disappears in the limit $\Gamma_{\rm sh}\ \sin\theta_B \rightarrow 0$ as a fraction

$$p \equiv \frac{1-\beta_{\rm sh}\cos\theta_B - (1/\Gamma_{\rm sh})\sin\theta_B}{1-\beta_{\rm sh}} \simeq (1-\Gamma_{\rm sh}\theta_B)^2 \qquad (52)$$

of the particles can propagate to upstream infinity (at least in the limit of a fully coherent magnetic field). This can be seen as follows. Particles cross the shock wave back towards downstream once their angle cosine with the shock normal becomes smaller than $\beta_{\rm sh}$. However, when $\Gamma_{\rm sh}\ \sin\theta_B < 1$, there exists a cone $\mathcal{C}_B$ around the magnetic field direction, of opening angle $\theta_B - {\rm acos}\ (\beta_{\rm sh})$, that never intersects the cone $\mathcal{C}$ defined around the shock normal with opening angle ${\rm acos}\ (\beta_{\rm sh})$. Because the pitch angle of the particles with respect to the magnetic field direction is conserved, particles that enter towards upstream in this cone $\mathcal{C}_B$ never recross the shock towards downstream (up to the influence of the turbulence). The fraction of particles that enter in this cone is approximately given by the ratio of the solid angles, i.e. the factor of $(1-\Gamma_{\rm sh}\ \theta_B)^2$ quoted before. Depending on the value of $\Gamma_{\rm sh}\ \theta_B$, this fraction can be substantial and these particles can excite plasma waves up to large distances from the shock. Of course, the actual precursor length remains finite as a result of the influence of large- and short-scale turbulence. In the following, we will simply discard these advection constraints in order to avoid introducing new parameters.

We also choose to discuss the limitations as a function of $X$ and $Y$, but at a fixed value of $\Gamma_{\rm sh}\ \sin\theta_B < 1$. The fact that $X \propto \Gamma_{\rm sh}$ and that $\Gamma_{\rm sh}\ \sin\theta_B$ is fixed modifies slightly the limitations derived previously. The main limitation for the oblique mode is the non-magnetization condition, $\mathcal{I}(\omega_{\rm obl.}) \gg \omega_{\rm ce}$ which can be rewritten $Y \ll GX^2$ as before. For the Weibel mode, the condition of non-magnetization of the protons, $\mathcal{I}(\omega_{\rm We.}) \gg \omega_{\rm ci}$ now reads $Y \ll (m_{\rm p}/m_{\rm e})^2 X^2$.

The Čerenkov resonant mode with longitudinal waves does not suffer any constraint in this parallel configuration, but the growth rate now becomes significantly smaller than that of the oblique mode (when the latter applies), by a factor of $\sin^{2/3}\theta_B$.

Concerning the Whistler modes, the condition $|\delta| < 1$ now leads to $Y \gg (m_{\rm e}/m_{\rm p})^{-2}\ (\Gamma_{\rm sh}\ \sin\theta_B)^{-2}\ X^4$. One recovers the condition expressed in the case of superluminal shock waves for $\sin\theta_B^2 \sim 1$, as one should. At a fixed value of $\Gamma_{\rm sh}\ \sin\theta_B$, however, the condition appears slightly different. Note that in the particular case of parallel shock waves, there is another non-trivial condition for these Whistler modes, which is related to the fact that the eigenfrequency $\omega_{\rm Wh.} \simeq \omega_{\rm ce}\ \sin\theta_B$ (at maximal growth) should exceed $\omega_{\rm ci}$, in order for the Whistler branch to apply. This translates into $X \ll \Gamma_{\rm sh}\ \sin\theta_B < 1$.

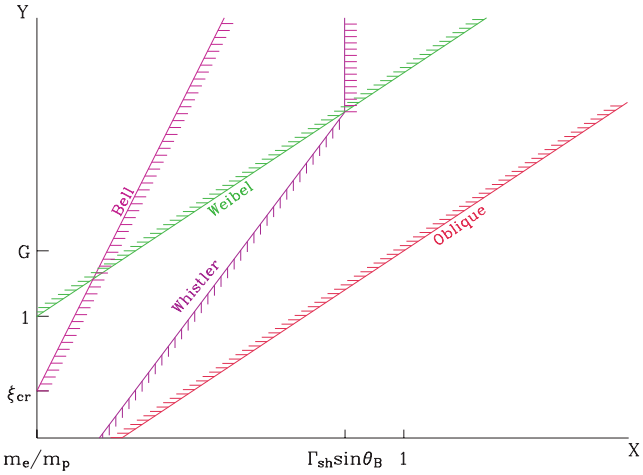


**Figure 2.** Same as Fig. 1 for the case of a parallel relativistic shock wave. The regions of growth are drawn at a fixed value of $\Gamma_{\rm sh}\ \sin\theta_B$ (here taken to be 0.3). The axes are plotted in log–log on arbitrary scale. The longitudinal mode can grow in all parameter space (in the idealized limit of a fully coherent upstream magnetic field) due to the divergence of the precursor length (see main text).

Finally, the Bell non-resonant instability requires the background protons to be magnetized, as noted in Section 4.2, which corresponds to $Y \gg \xi_{\rm cr}(m_{\rm p}/m_{\rm e})^6 X^6$.

These various conditions are expressed in Fig. 2, which is the analogue of Fig. 1 for parallel shock waves. Here as well, the limit of a pair shock can be obtained simply by taking the limit $m_{\rm e}/m_{\rm p} \rightarrow 1$ and discarding the Whistler branch as well as the Bell instability (which requires a net current to exist upstream).

As for the oblique shock wave, it is instructive to compare the present results to the simulations of Sironi & Spitkovsky (2009), who find in particular that instabilities can be triggered in parallel shocks for a magnetization $\sigma_{\rm SS} = 0.1$. Here, $\sigma_{\rm SS}$ corresponds to the definition of the magnetization given in Sironi & Spitkovsky (2009), or to our definition of downstream magnetization up to a factor of 3/4, the latter factor of 3/4 representing the difference between enthalpy and energy density for a relativistic gas. For a parallel shock wave, this thus corresponds to an upstream magnetization $\sigma_{\rm u} = 0.05\Gamma_{\rm sh}^2$, hence to $Y \simeq 0.05\Gamma_{\rm sh}^4\xi_{\rm cr}^{-1} \simeq 10^4\xi_{\rm cr}^{-1}$ for $X \simeq 20$. One may note that at this large level of magnetization, one has $\omega_{\rm ce} > \omega_{\rm pe}$. One can check immediately, using the above, that neither the oblique nor the Weibel instabilities can grow, as their respective non-magnetization conditions are not satisfied. The growth of instabilities observed in the simulations of Sironi & Spitkovsky (2009) is thus likely due to the Čerenkov resonance with the longitudinal modes that propagate along the magnetic field, which does not suffer from these constraints.

The above also allows to understand the abrupt transition as a function of shock obliquity: when $\sin\theta_B \rightarrow 1/\Gamma_{\rm sh}$, the growth of fluctuations is suddenly inhibited and so is Fermi acceleration. Indeed, as $\sin\theta_B \rightarrow 1/\Gamma_{\rm sh}$, the fraction of particles that can escape to upstream infinity vanishes, hence the precursor length now rapidly decreases to the value given by equation (5). This prevents the growth of fluctuations at high magnetization levels, as discussed

above for superluminal shock waves, and consequently this prevents successful Fermi acceleration (Lemoine et al. 2006).

## 6 TRIGGERING FERMI ACCELERATION

It is important to underline that Fig. 1 indicates whether instabilities triggered by the first generation of cosmic rays returning upstream have time to grow or not. If these instabilities cannot be triggered by the first generation, meaning if the shock wave characteristics are such that $(X, Y)$ lie above the thick solid line of Fig. 1, then instabilities cannot be triggered, either upstream or downstream (at least in the frame of our approach). Consequently Fermi cycles will not develop, at least for superluminal shock waves, in accordance with the arguments of Lemoine et al. (2006), Pelletier et al. (2009) and with the simulations of Niemiec et al. (2006).

If, however, the initial values of $X$ and $Y$ are such that instabilities can develop, Fig. 1 suggests that these instabilities will develop upstream and be transferred downstream. Fermi cycles may then develop provided the appropriate conditions discussed in Lemoine et al. (2006) and Pelletier et al. (2009) are satisfied. These conditions have been discussed under the assumption of isotropic short-scale magnetic turbulence, and we restrict ourselves to this assumption in the present work as well. It would certainly be interesting to generalize this discussion to more realistic turbulence configurations, as in Hededal et al. (2004), Dieckmann et al. (2006a) for instance. However, this clearly becomes more model dependent in terms of turbulence configuration and for this reason, we postpone such a study to future work.

Let us discuss first the case of upstream turbulence. When particles are scattered off short scale $\ell_c$, but intense magnetic fluctuations, the scattering frequency of a relativistic particle of momentum $p$ is

$$\nu_s \sim c\frac{e^2\langle\delta B^2\rangle}{p^2}\ell_c. \tag{53}$$

Since the oblique mode dominates over the Whistler and Weibel waves over most of the parameter space, one cannot ignore the influence of short-scale electrostatic fields. These electrostatic waves lead to a second order Fermi process in the upstream medium, with a concomitant pitch angle scattering. Indeed, the particle scatters against random electric fields $\pm E_\parallel$ along the shock normal ($\boldsymbol{x}$ direction), gaining momentum $\Delta p_\parallel \simeq \pm eE_\parallel\Delta t$, with $\Delta t \simeq \omega_p^{-1}$ at each interaction, and similarly in the perpendicular direction. The initial pitch angle of the particle (with respect to the shock normal) $\theta \ll 1$ in the upstream frame, and the particle is overtaken by the shock wave whenever $\theta \gtrsim 1/\Gamma_{sh}$ (Achterberg et al. 2001). This pitch angle diffuses according to

$$\frac{\langle\Delta\theta^2\rangle}{\Delta t} \simeq \frac{\langle\Delta p^2\rangle}{p^2\Delta t} \simeq e^2\frac{E_\perp^2 + 2\theta^2E_\parallel^2}{p_\parallel^2}\tau_c, \tag{54}$$

for a correlation time $\tau_c = \ell_c/c \sim \omega_{pe}^{-1}$. Therefore, we obtain a scattering rate similar to the previous one (53) in which the magnetic field fluctuation is replaced by the electric field fluctuation,

$$\nu_s' \sim c\frac{e^2\langle\delta E^2\rangle}{p^2}\ell_c. \tag{55}$$

This correspondence justifies that we treat the short-scale electric and magnetic fields on a similar footing and consider the total electromagnetic energy content. A conversion of a fraction of the energy of the beam into magnetic or electrostatic fluctuations is expected with $\xi_{em} < \xi_{cr}$, with typically $\xi_{cr} \sim 10^{-1}$ and $\xi_{em} \sim 10^{-2} - 10^{-1}$ (Spitkovsky 2008a). Scattering in the short-scale electromagnetic turbulence will govern the scattering process if it leads to $\langle\Delta p^2\rangle/p^2 \sim 1/\Gamma_{sh}^2$ on a time-scale $r_{L|B}/(\Gamma_{sh}\,c)$, with $r_{L|B}$ the Larmor radius of first generation cosmic rays as measured upstream relatively to the background magnetic field (see the corresponding discussion in Pelletier et al. 2009). If this short-scale turbulence governs the scattering process, then Fermi acceleration will operate. Assuming $\ell_c = c/\omega_{pe}$, this condition amounts to

$$\xi_{em} > \Gamma_{sh}\left(\frac{m_p}{m_e}\right)^{1/2}\sigma_u^{1/2}. \tag{56}$$

Using the fact that $\xi_{em} < \xi_{cr}$, this constraint can be rewritten as a bound on $\sigma_u$,

$$\sigma_u \ll \xi_{cr}^2\frac{m_e}{m_p}\Gamma_{sh}^{-2}. \tag{57}$$

This limit is very stringent indeed; in terms of our above parameters, it can rewritten as $Y \ll X\xi_{cr}/\Gamma_{sh}$. We will discuss the applicability of this inequality in concrete cases in the following section.

If this condition is not verified, the background unamplified magnetic field remains the main agent of particle scattering upstream. In this case, Fermi acceleration cycles can develop only if short-scale turbulence governs the scattering downstream of the shock wave. As discussed in Pelletier et al. (2009), this requires

$$\ell_{c|d} < r_{L|d} < \frac{\delta B_{|d}}{B_{|d}}\ell_{c|d}, \tag{58}$$

where all quantities should be evaluated in the downstream rest frame, and $r_{L|d}$ refers to the Larmor radius of the accelerated particles in this frame. This double inequality amounts to requiring that $\ell_{c|d}/c < \tau_s < \tau_{L,0}$, i.e. that the scattering time $\tau_s = \nu_s^{-1}$ be shorter than the Larmor time in the mean field $\tau_{L,0}$ in order to break the inhibition constraint of the mean field that tends to drag the particles in the downstream flow. The scattering must also develop in a special regime where the correlation time $\ell_{c|d}/c$ is shorter than the Larmor time. Regarding $\ell_{c|d}$, two main spatial scales are to be envisaged: the previous upstream electron skin depth, if one assumes that the typical scale of transverse fluctuations is preserved through shock crossing, and the downstream electron skin depth, if reorganization takes place through shock crossing. Assuming a typical electron temperature $\sim\Gamma_{sh}m_pc^2$ behind the shock, and accounting for shock compression of the electron density, this latter scale can actually be written as $c\,\omega_{pi}^{-1}$ ($\omega_{pi}$ the *upstream* ion plasma frequency), a factor 43 larger than the previous one. One should also envisage the possibility that the turbulence spectrum evolves to larger scales with time (Medvedev et al. 2005; Lemoine & Revenu 2006; Katz, Keshet & Waxman 2007), but we will not do so here. Let us consider the above two possibilities in turn.

If $\ell_{c|d} = c/\omega_{pe}$ (upstream electron skin depth), then the first inequality in equation (58) can be rewritten as $\xi_{em} < m_p/m_e$ and is therefore always satisfied. The second inequality amounts to $\sigma_d < (m_e/m_p)\xi_{em}^2$, hence $Y < \Gamma_{sh}\,X\,\xi_{em}^2/\xi_{cr}$. This latter inequality is much more stringent. If satisfied, it means that the downstream short-scale turbulence governs the scattering process, in particular it allows the particle to escape its orbit around the shock compressed background magnetic field on a time-scale smaller than the Larmor time in this field. This is a necessary condition for successful Fermi cycles.

If $\ell_{c|d} = c\,\omega_{pi}^{-1}$ (equivalently, the downstream electron skin depth), then the first inequality in equation (58) becomes $\xi_{em} < 1$, which is always true. The second inequality reads $\sigma_d < \xi_{em}^2$ (or $Y < \Gamma_{sh}^2\xi_{em}^2/\xi_{cr}$). We will summarize the above two possible cases for $\ell_{c|d}$ and parametrize the uncertainty on $\ell_{c|d}$ by writing the condition

as

$$\sigma_{\rm d} \ll \sigma_* \equiv \kappa\, \xi_{\rm em}^2, \tag{59}$$

with $\ell_{\rm c|d} = \kappa\, c/\omega_{pi}$ and $m_{\rm e}/m_{\rm p} \lesssim \kappa \lesssim 1$. One should, however, recall that the typical scale of electromagnetic fluctuations could evolve with the distance to the shock front, as envisaged in Medvedev et al. (2005), Lemoine & Revenu (2006) and Katz et al. (2007). This amounts to making $\kappa$ be a growing function of the energy taking values larger than 1. The above result clearly reveals the need for dedicated PIC simulations of shock wave at moderate magnetization, with realistic proton to mass ratio and geometry in order to reduce this large uncertainty on $\kappa$ and determine the precise conditions under which Fermi acceleration can take place.

To summarize this discussion, we obtain the following conditions for successful Fermi acceleration. If equation (57) is satisfied (or, to be more accurate, equation 56), then Fermi acceleration will operate because the short-scale fluctuations produced upstream is sufficiently intense to govern the scattering. In this case, it is important to stress that equation (5), which defines the length of the precursor, no longer applies. It should be replaced by equation (6), which is larger. Physically, the precursor widens, giving more time for the fluctuations to grow, thus reaching a higher efficiency in terms of $\xi_{\rm em}/\xi_{\rm cr}$. If equation (57) is not satisfied, e.g. because the upstream magnetization is not small enough, particles gyrate in the background magnetic field before experiencing the short-scale turbulence. Then Fermi acceleration will operate if equation (59) is verified. Consequently, a sufficient condition for the development of Fermi cycles is $\xi_{em} > (\sigma_{\rm crit}/\kappa)^{1/2}$, or equivalently $\sigma_* > \sigma_{\rm crit}$, where $\sigma_{\rm crit}$ is the maximum value of the upstream magnetization that allows turbulence to grow upstream and then be transferred downstream. As shown previously for a superluminal configuration, $\sigma_{\rm crit} = \Gamma_{\rm sh}^{-3}\, \xi_{\rm cr} m_{\rm p}/m_{\rm e}$ for an electron–proton plasma in the realistic case where $\Gamma_s \lesssim 150 \xi_{\rm cr}^{1/3}$ so that the transition is governed by the excitation of whistler waves; or $\sigma_{\rm crit} = \Gamma_{\rm sh}^{-2} \xi_{\rm cr}^{2/3} (m_{\rm p}/m_{\rm e})^{1/3}$ for an electron–positron plasma, with the development of the oblique two stream instability. The spectral index and the maximal energy remain to be determined however. In this respect, we note that equation (58) provides an upper bound for this maximal energy: $\epsilon_{\rm max} \simeq \Gamma_{\rm sh} m_{\rm p} c^2 (\sigma_*/\sigma_{\rm u})^{1/2}$ in the front frame.

The more likely development of the Fermi process is thus hybrid, in the sense that it is of drift type upstream and of diffusive type downstream. As Fermi cycles develop, particles are accelerated beyond the energy $\Gamma_{\rm sh}^2 m_{\rm p} c^2$ considered here for the first generation. Although they are less numerous, they stream farther ahead of the shock and are therefore liable to induce stronger amplification. One can only speculate about these issues, since the spectral index depends strongly on the assumption made on the shape of the turbulence spectra, upstream as well as downstream. In particular, if the magnetic field amplified downstream through the Weibel instability decays on scales of order of tens or hundreds of electron inertial lengths $\delta_{\rm e}$, the particles will likely escape towards downstream because of the lack of scattering agents, thereby cutting off the Fermi process prematurely. Nevertheless, assuming for the sake of discussion that Fermi cycles develop with a spectral index $s \sim 2$–$3$, the number density of cosmic rays streaming upstream scales as $n_{\rm b|u}(> p_*) \propto (p_*/p_0)^{1-s}$, with $p_0 \sim \Gamma_{\rm sh}^2 m_{\rm p} c^2$. The beam plasma frequency, which controls the growth rates of the instabilities, $\omega_{\rm p*}(> p_*) \propto (p_*/p_0)^{-s/2}$, whereas the precursor length $\ell_{\rm F|u}(> p_*) \propto (p_*/p_0)$. Since the growth rates of the resonant instabilities which develop upstream scale as $\omega_{\rm p*}^{2/3}$, $s < 3$ would guarantee that the growth factor of the instabilities triggered by these high-energy particles exceeds that for the first generation. These findings seem in agreement with the numerical simulations of Keshet et al. (2009) and Sironi & Spitkovsky (2009) who observe wave growth farther from the shock from high-energy particles, as time increases.

### 6.1 Applications

It is interesting to situate the relativistic shock waves of physical interest in the above diagram. Here, we consider three proto-typical cases: a pulsar wind, a gamma-ray burst external shock waves expanding in the interstellar medium, and a gamma-ray burst external shock wave propagating along a density gradient in a Wolf–Rayet wind. We find the following.

(i) Pulsar winds: with $\Gamma \simeq 10^6$ and $\sigma_{\rm u} \simeq 0.01$, one finds $(X, Y) \sim (500,\, 10^{10}\, \xi_{\rm cr}^{-1})$; the level of magnetization is thus so high that no wave can grow, either upstream or downstream. Fermi acceleration should consequently be inhibited.

(ii) Gamma-ray burst external shock waves expanding in the interstellar medium: for $\Gamma \simeq 300$ and $\sigma_{\rm u} \sim 10^{-9}$ (i.e. $B \sim 3\,\mu$G), one finds $(X, Y) \sim (0.1,\, 10^{-5}\, \xi_{\rm cr}^{-1})$. Wave growth should be efficient both upstream and downstream. Concerning Fermi acceleration, equation (57) amounts to $Y < \xi_{\rm cr} m_{\rm e}/m_{\rm p}$. It can thus be only marginally satisfied. However, equation (59) is most likely satisfied, so that Fermi acceleration should develop, even in the early afterglow phase when $\Gamma_{\rm sh} \sim 300$.

(iii) Gamma-ray burst external shock waves propagating along a density gradient in a Wolf–Rayet wind: taking a surface magnetic field of $1000\,G$ for a $10\,{\rm R}_\odot$ Wolf–Rayet progenitor, the magnetization at distances of $10^{17}$ cm is $\sigma_{\rm u} \sim 10^{-4}$ (Crowther 2007). This gives $(X, Y) \sim (0.1,\, \xi_{\rm cr}^{-1})$. Growth may or may not occur in this case, depending on the precise values of $\Gamma_{\rm sh}$, $\sigma_{\rm u}$ and $\xi_{\rm cr}$. In detail, the condition for Weibel growth $Y \lesssim 1$ is likely not verified for the above fiducial values, but could be verified in less magnetized winds and at later stages of evolution, with a smaller value of $\Gamma_{\rm sh}$. The condition for growth of Whistler waves, $Y \lesssim 1/X$, may be satisfied if $\xi_{\rm cr} \gtrsim 0.1$ and it is likely to be more easily verified at smaller values of $\Gamma_{\rm sh}$ and $\sigma_{\rm u}$. Finally, the (most stringent) condition for growth of the oblique mode, equation (50), is likely not verified in the initial stages with $\Gamma_{\rm sh} \simeq 300$ and the above fiducial value of $\sigma_{\rm u}$, but would be verified if $\sigma_{\rm u}$ was smaller.

However, equation (57) cannot be satisfied in this case, meaning that the orbit of the particle upstream is governed by the wind magnetic field, not by the amplified short-scale component. Regarding the bound equation (59), it can be satisfied, depending on the values of the wind magnetization and most particularly on the value of $\kappa$. The possibility of Fermi acceleration thus remains open in this case. More work is necessary to understand the properties of downstream turbulence in order to determine whether particle can eventually be accelerated.

### 6.2 Further considerations

It is important to emphasize that we do not understand yet the structure of a relativistic shock front in detail. In the previous section, we have assumed that the shock front is structured like a non-relativistic front and just extended the non-relativistic results. Since MHD compressive instability and extraordinary ionic modes can be excited, we cannot exclude that the foot be full of relativistically hot protons and electrons of similar temperature $\bar{\gamma} m_{\rm p} c^2$ with $1 \ll \bar{\gamma} \leq \Gamma_s$. In that case the plasma response would be different because the intermediate whistler range (and also extraordinary range) would

disappear so that the plasma would behave like a relativistic pair plasma. Then, the relevant instabilities are the Weibel and oblique modes (in the unmagnetized approximation). The length of the precursor and the Weibel growth rate remain unchanged, hence the domain of growth of the Weibel instability also remains unchanged. The growth rate of the oblique mode is, however, reduced because the background plasma frequency is smaller by a ratio $(\gamma m_{\rm p}/m_{\rm e})^{1/2}$. Therefore, the condition of growth on the advection time-scale now reads $Y \ll \xi_{\rm cr}^{-1/3}\,\Gamma_{\rm sh}^{1/3}\,X^{-1/3}\,(\gamma m_{\rm p}/m_{\rm e})^{-1/3}$. The ratio of the growth rates of the oblique mode to the Weibel mode can be written as $(\gamma\xi_{\rm cr})^{-1/6}$, hence the Weibel instability becomes the dominant mode if $\gamma \gg \xi_{\rm cr}^{-1}$.

In the downstream plasma, the magnetic fluctuations generated by the Weibel instability are expected to disappear rapidly because they do not correspond to plasma modes. Whistler and other resonant eigenmodes (when they are excited) are, however, transmitted and although they are not excited downstream, their damping is weak. When Fermi cycles develop, they create 'inverted' distribution downstream, that should produce a maser effect.

Tangled magnetic field carried by the upstream flow are very compressed downstream and thus opposite polarization field lines come close together. This should produce magnetic reconnections in an unusual regime where protons and electrons have a similar relativistic mass of order $\Gamma_{\rm sh}m_{\rm p}c^2$. Such a regime of reconnection deserves a specific investigation with appropriate numerical simulations. Despite magnetic dissipation, reconnections would probably create a chaotic flow that favours diffusion of particles from downstream to upstream.

## 7 CONCLUSIONS

In this work, we have carried out a detailed study of the micro-instabilities at play in the precursor of a ultra-relativistic shock wave. The main limitation for the growth of these waves is related to the length of precursor, which is itself related to the level of magnetization in the upstream plasma (where magnetization refers to the background field, not the shock generated short-scale fields). Nevertheless, we have found electronic and ionic instabilities that grow sufficiently fast in the precursor of a relativistic shock. The fastest growing instabilities are due to the Čerenkov resonance between the beam of accelerated (and shock reflected protons) and the upstream plasma Whistler waves and electrostatic modes. The Weibel instability, which is non-resonant by essence, is also excited, but its growth is generally superseded by that of the previous modes. The strongest amplification occurs on very short spatial scales $\sim\delta_{\rm e}$, the electron skin depth in the upstream plasma. Our results are summarized in Fig. 1 for the generic case of relativistic superluminal shock waves, which delimits the domains in which electromagnetic modes are excited in terms of shock Lorentz factor and upstream magnetization and defines the critical value $\sigma_{\rm crit}$ of the magnetization below which Fermi process can operate. Fig. 2 presents the corresponding limitations for the case of parallel shock waves; in this case, the growth of instabilities is made much easier by the divergence of the precursor length for a fraction of the particles returning upstream. Our results explain some features of recent PIC simulations of relativistic pair shocks of various geometries and magnetization levels.

We have discussed the conditions under which Fermi acceleration can proceed superluminal shock waves once a significant fraction of the cosmic ray energy has been dumped into these short-scale electromagnetic fluctuations. Fermi acceleration can operate if the upstream magnetization ($\sigma_{\rm u}$) or downstream magnetization ($\sigma_{\rm d}$) is low enough for the shock generated turbulence to govern the scattering of particles. This is the second condition that states the required level of electromagnetic energy density versus the magnetization. This requires either $\sigma_{\rm u} \ll \xi_{\rm em}^2\,(m_{\rm e}/m_{\rm p})\Gamma_{\rm sh}^{-2}$ (for upstream scattering), which is however difficult to fulfil, or $\sigma_{\rm d} \ll \kappa\xi_{\rm em}^2$ (for downstream scattering, which is easily fulfilled with a low level of turbulence); $\xi_{\rm em}$ indicates the fraction of incoming energy transferred into electromagnetic fluctuations, with $\xi_{\rm em} \sim 10^{-2}$–$10^{-1}$ generally indicated by PIC simulations, and $\kappa$ is a fudge factor that encaptures our ignorance of the transfer of electromagnetic modes excited upstream through the shock, $m_{\rm e}/m_{\rm p} \lesssim \kappa \lesssim 1$ (and it may be even larger depending on the particle energy if the scale of the electromagnetic fluctuations evolves with the distance to the shock). We emphasize the need for PIC simulations with realistic geometry, realistic proton to electron mass ratios and moderate magnetization (of order of the above) in order to lift this uncertainty on $\kappa$ and to determine the precise conditions under which Fermi acceleration can take place. This limitation also places a strict upper bound on the maximum energy that is achievable through the Fermi process, namely $\epsilon_{\rm max} \simeq \Gamma_{\rm sh}m_{\rm p}c^2\,(\sigma_{\rm crit}/\sigma_{\rm u})^{1/2}$, with $\sigma_{\rm crit}$ the maximum magnetization that allows waves to grow, and $\sigma_{\rm u}$ the upstream background magnetization (see discussion after equation (59). Beyond this intrinsic limit, the scattering time indeed becomes longer than the Larmor time in the mean field downstream, so that the particle is advected downstream by the mean field and Fermi cycles end.

We have also applied our calculations to several cases of astrophysical interest. In practice, we find that terminal shocks of pulsar winds have a magnetization level that is too high to allow for the amplification of short-scale electromagnetic fields, so that particle acceleration must be inhibited. We have found that gamma-ray burst external shock waves propagating into a typical interstellar medium should lead to strong amplification of the magnetic field and to Fermi cycles, even at high Lorentz factor. The energies reached by the suprathermal electrons can easily explain the afterglow emission through jitter radiation (Medvedev 2000). However, if the shock wave propagates in a stellar wind, the upstream magnetization may be too large to allow for particle acceleration, even though magnetic field amplification should take place.

## ACKNOWLEDGMENTS

We warmly acknowledge A. Marcowith for collaboration at an earlier stage of this work and for a careful reading of the manuscript. We also thank the referee for a detailed reading of the manuscript and for useful suggestions. One of us (GP) acknowledges fruitful discussions with J. Arons, A. Bell, L. Drury, J. Kirk, Y. Lyubarsky, J. Niemiec, M. Ostrowski, B. Reville, H. Völk, A. Spitkovsky and L. Sironi.

## REFERENCES

Achterberg A., Wiersma J., 2007, A&A, 475, 19
Achterberg A., Gallant Y., Kirk J. G., Guthmann A. W., 2001, MNRAS, 328, 393
Achterberg A., Wiersma J., Norman C. A., 2007, A&A, 475, 1
Bednarz J., Ostrowski M., 1998, Phys. Rev. Lett., 80, 3911
Bell A., 2004, MNRAS, 353, 550
Bell A., 2005, MNRAS, 358, 181
Blandford R., McKee C., 1976, Phys. Fluids, 19, 1130
Bret A., 2009, ApJ, 699, 990
Bret A., Firpo M.-C., Deutsch C., 2004, Phys. Rev. E, 70, 046401
Bret A., Firpo M.-C., Deutsch C., 2005a, Phys. Rev. Lett., 94, 115002
Bret A., Firpo M.-C., Deutsch C., 2005b, Phys. Rev. E, 72, 016403

Chang P., Spitkovsky A., Arons J., 2008, ApJ, 674, 378
Couch S. M., Milosavljević M., Nakar E., 2008, ApJ, 688, 462
Crowther P. A., 2007, ARA&A, 45, 177
Dieckmann M. E., 2005, Phys. Rev. Lett., 94, 155001
Dieckmann M. E., Eliasson B., Shukla P. K., 2004a, Phys. Rev. E, 70, 036401
Dieckmann M. E., Eliasson B., Shukla P. K., 2004b, ApJ, 617, 1361
Dieckmann M. E., Drury L. O., Shukla P. K., 2006a, New J. Phys., 8, 40
Dieckmann M. E., Shukla P. K., Drury L. O., 2006b, MNRAS, 367, 1072
Dieckmann M. E., Shukla P. K., Drury L. O., 2008, ApJ, 675, 586
Ellison D. C., Double G. P., 2004, Astropart. Phys., 22, 323
Frederiksen J. T., Dieckmann M. E., 2008, Phys. Plasmas, 15, 094503
Frederiksen J. T., Hededal C. B., Haugbølle T., Nordlund Å, 2004, ApJ, 608, L13
Gallant Y., Achterberg A., 1999, MNRAS, 305, L6
Gruzinov A., Waxman E., 1999, ApJ, 511, 852
Hededal C. B., Haugbølle T., Frederiksen J. T., Nordlund Å, 2004, ApJ, 617, L107
Hededal C. B., Nishikawa K.-I., 2005, ApJ, 623, L89
Kato T. N., 2007, ApJ, 668, 974
Katz B., Keshet U., Waxman E., 2007, ApJ, 655, 375
Keshet U., Waxman E., 2005, Phys. Rev. Lett., 94, 111102
Keshet U., Katz B., Spitkovsky A., Waxman E., 2009, ApJ, 693, L127
Kirk J. G., Guthmann A. W., Gallant Y. A., Achterberg A., 2000, ApJ, 542, 235
Lemoine M., Pelletier G., 2003, ApJ, 589, L73
Lemoine M., Revenu B., 2006, MNRAS, 366, 635
Lemoine M., Pelletier G., Revenu B., 2006, ApJ, 645, L129
Li Z., Waxman E., 2006, ApJ, 651, L328
Lyubarsky Y. E., 2002, in Becker W., Lesch H., Trümper J., eds, Proc. 270 WE-Heraeus Seminar on Neutron Stars, Pulsars, and Supernova Remnants. MPE, Garching, p. 230
Lyubarsky Y., Eichler D., 2006, ApJ, 647, L1250
Medvedev M. V., 2000, ApJ, 540, 704
Medvedev M. V., Loeb A., 1999, ApJ, 526, 697
Medvedev M. V., Fiore M., Fonseca R. A., Silva L. O., Mori W. B., 2005, ApJ, 618, L75
Medvedev M. V., Zakutnyaya O. V., 2009, ApJ, 696, 2269
Melrose D. B., 1986, Instabilities in Space and Laboratory Plasmas. Cambridge Univ. Press, Cambridge
Milosavljević M., Nakar E., 2006, ApJ, 651, 979
Niemiec J., Ostrowski M., 2004, ApJ, 610, 851
Niemiec J., Ostrowski M., 2006, ApJ, 641, 984
Niemiec J., Ostrowski M., Pohl M., 2006, ApJ, 650, 1020
Nishikawa K.-I., Hardee P., Richardson G., Preece R., Sol H., Fishman G. J., 2003, ApJ, 595, 555
Nishikawa K.-I., Hardee P., Richardson G., Preece R., Sol H., Fishman G. J., 2005, ApJ, 622, 927
Nishikawa K.-I., Hardee P. E., Hededal C. B., Fishman G. J., 2006, ApJ, 642, 1267
Nishikawa K.-I., Hededal C. B., Hardee P. E., Fishman G. J., Kouveliotou C., Mizuno Y., 2007, Astrophys. Space Sci., 307, 319
Ohira Y., Reville B., Kirk J. G., Takahara F., 2009, ApJ, 698, 445
Pelletier G., Lemoine M., Marcowith A., 2009, MNRAS, 393, 587
Piran T., 2005, Rev. Mod. Phys., 76, 1143
Reville B., Kirk J. G., Duffy P., 2006, Plasma Phys. Control. Fusion, 48, 1741
Riquelme M. A., Spitkovsky A., 2009, ApJ, 694, 626
Silva L. O., Fonseca R. A., Tonge J. W., Dawson J. M., Mori W. B., Medvedev M. V., 2003, ApJ, 596, L121
Spitkovsky A., 2005, in Bulik T., Rudak B., Madejski G., eds, AIP Ser. Vol. 801, Astrophysical Sources of High Energy Particles and Radiation. Am. Inst. Phys., New York, p. 345
Sironi L., Spitkovsky A., 2009, ApJ, 698, 1523
Spitkovsky A., 2008a, ApJ, 673, L39
Spitkovsky A., 2008b, ApJ, 682, L5
Treumann R. A., Jaroschek C. H., 2008a, preprint (arXiv:0805.2132)
Treumann R. A., Jaroschek C. H., 2008b, preprint (arXiv:0805.2162)
Waxman E., 1997, ApJ, 485, L5
Wiersma J., Achterberg A., 2004, A&A, 428, 365

This paper has been typeset from a TEX/LATEX file prepared by the author.